

# Interfacial reaction kinetics

 B. O’Shaughnessy<sup>1,a</sup> and D. Vavylonis<sup>2,b</sup>
<sup>1</sup> Department of Chemical Engineering, Columbia University, 500 West 120th Street, New York, NY 10027, USA

<sup>2</sup> Department of Physics, Columbia University, 538 West 120th Street, New York, NY 10027, USA

Received 8 June 1998 and Received in final form 10 September 1999

**Abstract.** We study irreversible A–B reaction kinetics at a fixed interface separating two immiscible bulk phases, A and B. Coupled equations are derived for the hierarchy of many-body correlation functions. Postulating physically motivated bounds, closed equations result without the need for *ad hoc* decoupling approximations. We consider general dynamical exponent  $z$ , where  $x_t \sim t^{1/z}$  is the rms diffusion distance after time  $t$ . At short times the number of reactions per unit area,  $\mathcal{R}_t$ , is *2nd order* in the far-field reactant densities  $n_A^\infty, n_B^\infty$ . For spatial dimensions  $d$  above a critical value  $d_c = z - 1$ , simple mean field (MF) kinetics pertain,  $\mathcal{R}_t \sim Q_b t n_A^\infty n_B^\infty$  where  $Q_b$  is the local reactivity. For low dimensions  $d < d_c$ , this MF regime is followed by 2nd order diffusion controlled (DC) kinetics,  $\mathcal{R}_t \approx x_t^{d+1} n_A^\infty n_B^\infty$ , provided  $Q_b > Q_b^* \sim (n_B^\infty)^{[z-(d+1)]/d}$ . Logarithmic corrections arise in marginal cases. At long times, a cross-over to *1st order* DC kinetics occurs:  $\mathcal{R}_t \approx x_t n_A^\infty$ . A density depletion hole grows on the more dilute A side. In the symmetric case ( $n_A^\infty = n_B^\infty$ ), when  $d < d_c$  the long time decay of the interfacial reactant density,  $n_A^s$ , is determined by fluctuations in the initial reactant distribution, giving  $n_A^s \sim t^{-d/(2z)}$ . Correspondingly, A-rich and B-rich regions develop at the interface analogously to the segregation effects established by other authors for the bulk reaction  $A + B \rightarrow \emptyset$ . For  $d > d_c$  fluctuations are unimportant: local mean field theory applies at the interface (joint density distribution approximating the product of A and B densities) and  $n_A^s \sim t^{(1-z)/(2z)}$ . We apply our results to simple molecules (Fickian diffusion,  $z = 2$ ) and to several models of short-time polymer diffusion ( $z > 2$ ).

**PACS.** 05.40.-a Fluctuation phenomena, random processes, noise, and Brownian motion –  
 68.45.Da Adsorption and desorption kinetics; evaporation and condensation –  
 82.35.+t Polymer reactions and polymerization

## 1 Introduction

In a large class of chemically reacting systems, irreversible bimolecular reactions occur at a permanent interface separating two bulk phases. Reactive molecules in one phase are able to react with molecules in the other phase only; hence reaction events can occur within the limits of the narrow interfacial region only. A number of technologically important examples [1,2] entail small molecules reacting at liquid-liquid, liquid-gas or liquid-solid interfaces. In the present study we address interfaces which are fixed in space and do not broaden as reactions proceed; the two bulk phases do not mix with one another. However, the physics we will explore may provide insight to the very different problem of non-stationary reactive fronts where chemical reactions occur at a moving and possibly broadening interface separating miscible phases [3–11].

Another important class of reactive interfacial systems involves macromolecules. Of particular technological significance is the process of reactive blending [12,13] where

the compatibilization of two immiscible polymer melts A and B is assisted by attaching reactive groups to a certain fraction of the chains. The A–B copolymers generated by reactions, which can occur at the A–B melt interface only, serve both to reinforce the interface [14,15] and to promote the mechanical mixing of the two melts [13,16].

The manner in which reaction kinetics are modified by the presence of an interface is a fundamental issue within the general field of chemical reaction kinetics. Despite this, and despite the numerous applications such as those mentioned above, no complete and systematic theory exists. We emphasize that each reaction event necessitates the simultaneous arrival, at the same location within the interface, of two molecular species A and B, one from each bulk phase. (This is very different to the problem [17,18] of a single bulk adjacent to a homogeneous “reactive interface” where each “reaction” event, *e.g.* the irreversible adsorption of a molecule onto a solid surface, requires the arrival of only *one* molecule at the interface.) The interfacial reaction kinetics which are the subject of the present paper were theoretically studied for the case of small molecules by Durning and O’Shaughnessy [19], and the end-functionalized polymer case by O’Shaughnessy

---

<sup>a</sup> e-mail: bo8@columbia.edu

<sup>b</sup> e-mail: dvav@phys.columbia.edu

and Sawhney [20,21] and Fredrickson [22]. These theories in fact described a certain short time regime only, for systems where the reacting species are dilute in an unreactive background. Fredrickson and Milner [23] argued that at later times different kinetic behaviors onset, with forms dependent on reactive species concentration.

In this paper we develop a near-exact theory of irreversible interfacial reaction kinetics. We calculate time-dependent reaction rates as a function of density and local reactivity of the reactive species. In addition, density profiles on either side of the interface are determined. A short version of the present manuscript has appeared [24]. Our framework is quite general in terms of the diffusive dynamics of the reactive species, as defined by the dynamical exponent,  $z$ :

$$x_t = a \left( \frac{t}{t_a} \right)^{1/z}, \quad (1)$$

where  $x_t$  is the rms displacement of a reactive group after time  $t$ . Here  $a$  is the linear dimension of the reactive species A and B, and  $t_a$  is the diffusion time corresponding to  $a$ . Thus, setting  $z = 2$  in our results yields reaction rates for small molecules obeying Fick's diffusion law. As a second example, if one seeks the short time reaction kinetics of small reactive groups attached to polymer chains in the melt, then appropriate values would be  $z = 4$  or  $z = 8$ , depending on the time regime and degree of entanglement [25,26].

This study will always assume the interface is clean. Thus we ignore effects associated with accumulation of A–B reaction products at the interface whose presence may eventually diminish reaction rates [20,21,23].

### Bulk kinetics (A+B → 0): a brief review

Before attacking the present interfacial problem, it is helpful to consider first the analogous and somewhat simpler problem in the *bulk*, where irreversible bimolecular reactions between A and B, generating inert products, can occur anywhere within a single bulk phase. There are no A–A or B–B reactions. For the small molecules case,  $z = 2$ , many well-established results exist (“A + B → 0”) [27–31]. Suppose A and B have equal diffusivities and are initially uniformly distributed with equal densities  $n(0)$  within some solvent. (The case  $n(0) = 1/a^d$  would correspond to every molecule being reactive; generally  $n(0) \leq 1/a^d$ .) Reactions are now “switched on” at  $t = 0$ . Then, whenever an A and a B particle collide (*i.e.* approach to within distance of order  $a$  of one another) they react irreversibly with probability  $Q_b$  per unit time, where  $Q_b$  is the local reactivity. For simplicity, let us confine our bulk discussion to “infinitely” reactive particles; reaction then occurs every time an A–B pair collides. This corresponds to setting [32]  $Q_b = 1/t_a$  (the effective local reactivity cannot exceed the rate,  $1/t_a$ , at which diffusion can bring two reactive species together). Our discussion will consider a general spatial dimensionality  $d$ .

What are the reaction kinetics in this bulk system? What are the time dependencies of the number of reactions per unit volume which have occurred after time  $t$ , namely  $\mathcal{R}_t^{\text{bulk}}$ , and the reactant density  $n(t)$ ? The simplest guess is that mean field (MF) theory applies: this amounts to assuming reactants are always distributed as in *equilibrium*. Hence the reaction rate equals the *equilibrium* density of A–B pairs in contact, multiplied by  $Q_b$ . Thus,  $\dot{\mathcal{R}}_t^{\text{bulk}} \equiv (d/dt)\mathcal{R}_t^{\text{bulk}} = Q_b a^d n^2(t) = (a^d/t_a)n^2(t)$ . Now this MF prediction is in fact valid only for sufficiently large  $d$  such that diffusion is effective in dissipating reaction-induced non-equilibrium spatial correlations. The maximum number of A–B pairs which diffusion can have brought together by the time  $t$  increases as  $x_t^d \sim t^{d/z}$ ; provided  $d > z$ , this is sufficient to restore the depletion, which would arise in the two-body correlation function, due to reactions as implied by the MF prediction,  $\mathcal{R}_t^{\text{bulk}} \sim t$ . But for lower dimensions,  $d < z$ , since diffusion cannot supply material fast enough to keep pace with this reaction rate, equilibrium spatial correlations are destroyed: a depletion hole of size  $x_t$  grows in the A–B 2-body correlation function. Reaction kinetics are then very different; for short times  $\mathcal{R}_t^{\text{bulk}} \approx x_t^d n^2(0)$  is the number of reactive pairs initially within diffusive range of one another, *i.e.* whose initial separations were less than  $x_t$ . In summary, for times short enough that the relative density drop is small,  $n(t) \approx n(0)$ , we have

$$\begin{aligned} \dot{\mathcal{R}}_t^{\text{bulk}} &= -\frac{dn(t)}{dt} = k^{\text{bulk}} n^2(t), \\ k^{\text{bulk}}(t) &\approx \begin{cases} a^d/t_a & d > z \\ dx_t^d/dt \sim t^{d/z-1} & d < z \end{cases} \end{aligned} \quad (\text{short times}). \quad (2)$$

These are second order rate kinetics, with a rate constant,  $k^{\text{bulk}}$ , which is time-dependent for low dimensions  $d < z$ .

The two classes of kinetics in equation (2) reflect the fact that reactive groups explore space “compactly” in low dimensions [33–35]: for  $d < z$  it is simple to show that (in the absence of reactions) the number of collisions between an A–B pair, with some given initial separation, increases for large times as  $\sim t^{1-d/z}$ . Thus reaction is inevitable by the time  $t$  for any reactive pair initially separated by  $x_t$  or less. By contrast, for  $d > z$  space is explored in a “non-compact” or dilute fashion; with finite probability, the same two particles may avoid collision as  $t \rightarrow \infty$ . This survival probability is an increasing function of the initial separation. Reaction is no longer inevitable between all pairs within diffusive range, and MF theory applies [32,36]. For the interface problem, we will find a similar division between compact and non-compact reaction kinetics, but now at a dimension  $d + 1 = z$ . Indeed, the short time interface kinetics turn out to be analogous to those of a  $(d + 1)$ -dimensional bulk problem [19–21].

Equation (2) describes the short time kinetics. What happens at very long times? For  $d > z$  one might anticipate the MF kinetics of equation (2) would continue indefinitely, implying  $n \sim 1/t$  asymptotically. In fact,

for two-species A–B systems this is true only for very high dimensions,  $d > 2z$ . This was demonstrated for  $z = 2$  by Ovchinnikov and Zeldovich [27] and by Toussaint and Wilczek [28]. These authors showed that in lower dimensions fluctuations in the initial density distribution determine the asymptotic form of  $n(t)$ . Their argument, generalized to arbitrary  $z$ , is roughly as follows. Consider a portion of the reacting system of volume  $\Omega$  and let  $N_A(t), N_B(t)$  be the number of unreacted A and B particles in this region at time  $t$ . Assuming random initial spatial distributions of A and B, the initial fluctuations of  $N_A(0)$  and  $N_B(0)$ , about their mean value  $n(0)\Omega$ , will be of order  $\sqrt{n(0)\Omega}$ . (Note that  $n(t)$  is the *mean* density after time  $t$ .) Of the same order will be the fluctuations in  $\delta N_0 \equiv N_A(0) - N_B(0)$ , the average value of which is zero. As reactions proceed, fluctuations will diminish. However, since reaction events conserve the difference between the number of A and B particles, fluctuations in  $\delta N_t \equiv N_A(t) - N_B(t)$  can decay by diffusion only. Thus, if we consider small regions,  $\Omega < x_t^d$ , then by time  $t$  the initial difference of order  $\delta N_0$  has had sufficient time to decay away due to diffusion. But for large regions,  $\Omega > x_t^d$ , the difference must be close to its original value,  $\delta N_t \approx \delta N_0$ . Roughly, then, in a region of volume  $x_t^d$ , the total number of reactants cannot be smaller than a number of the order of  $\sqrt{n(0)x_t^d}$ . It follows that the density cannot decay faster than  $n(t) \approx \sqrt{n(0)x_t^d}/x_t^d \sim \sqrt{n(0)}t^{-d/(2z)}$ . For  $d < 2z$ , this is a slower decay than the MF  $t^{-1}$  prediction, and one concludes that this diffusive relaxation of initial fluctuations then governs the long time decay. To summarize,

$$n(t \rightarrow \infty) \sim \begin{cases} t^{-1} & d > 2z \\ t^{-d/2z} & d < 2z \end{cases} \quad (\text{bulk}). \quad (3)$$

For interfacial reactions, we will establish a rather similar long time fluctuation-dominated decay of densities near the interface for sufficiently small  $d$ . Analogously to the bulk case, this is accompanied by segregation of reactants into A-rich and B-rich domains of size  $x_t$  in the region adjacent to the interface.

### Interfacial kinetics: scaling arguments

Let us turn now to the interface problem, shown schematically in Figure 1. We consider two  $d$ -dimensional bulk phases containing, respectively, reactive species A and B with initial densities  $n_A^\infty$  and  $n_B^\infty$ . The reactants are of size  $a \leq h$ , where  $h$  is the width of the thin  $(d-1)$ -dimensional interfacial region which is the locus of all reaction events. We assume A and B have identical diffusion dynamics. To begin, consider the symmetric case  $n_A^\infty = n_B^\infty \equiv n$  and the infinitely reactive limit,  $Q_b \rightarrow 1/t_a$  (every A–B collision produces a reaction).

The short time reaction kinetics of this interfacial system are analogous to those of a  $(d+1)$ -dimensional bulk problem. To see this, consider how many degrees of freedom are needed to specify the ‘‘reaction rate’’ for a single

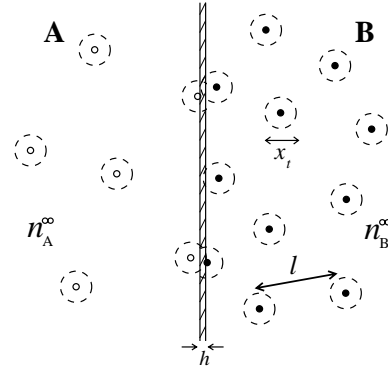


**Fig. 1.** Two bulk phases A and B, separated by a thin interface of width  $h$ , contain diffusing reactants A and B with densities  $n_A^\infty, n_B^\infty$ . Reactions between A and B molecules, generating inert products, may occur in the interfacial region only. The typical distance between reactants on the B side is  $l = a(n_B^\infty a^d)^{-1/d}$ . During short time 2nd order diffusion-controlled kinetics regimes, the reaction rate is determined by the small fraction of A–B pairs which were initially close enough to have diffused and met within time  $t$ . That is, reactions are confined to those pairs whose exploration volumes (indicated by dashed lines) overlap at time  $t$ . Note that such pairs must be within  $x_t$  of the interface.

A–B pair. One coordinate must specify how far from the interface particle A lies, and similarly for B. A further  $d-1$  coordinates must specify their relative location, giving  $d+1$  degrees of freedom [19] in total. That is, there are  $d+1$  diffusive degrees of freedom which must vanish in order that an A–B pair may react. These are the reaction conditions for a  $(d+1)$ -dimensional bulk diffusion-reaction problem, and similar reasoning to that for the bulk dictates that non-compact MF kinetics pertain for  $d+1 > z$ , whilst for  $d+1 < z$  the kinetics are of compact diffusion-controlled (DC) form. Thus the reaction rate per unit interface area,  $\mathcal{R}_t$ , obeys 2nd order rate kinetics with a 2nd order rate constant  $k^{(2)}$ :

$$\mathcal{R}_t = k^{(2)}n^2, \quad k^{(2)}(t) \approx \begin{cases} ha^d/t_a & d+1 > z \\ dx_t^{d+1}/dt \sim t^{(d+1)/z-1} & d+1 < z \end{cases} \quad (\text{short times, } Q_b t_a = 1) \quad (4)$$

in complete analogy to equation (2) for the bulk problem, but with  $d$  replaced by  $d+1$ . The mean field result for  $d+1 > z$  follows because in equilibrium there are  $ha^d n^2$  A–B pairs in contact per unit area of interface<sup>1</sup>. The DC compact kinetics are determined by the small fraction (at short times) of A–B pairs which were initially separated by less than  $x_t$ ; for  $d+1 < z$  any such pair will definitely have reacted by time  $t$ . The number of such A–B pairs per unit interfacial area is  $x_t^{d+1} n^2$  (see Fig. 1). Note that the

<sup>1</sup> A slight complication here, which will be addressed in Section 6, is that this result is modified when  $z < d+1 < z+1$ ; in that case  $k^{(2)} \approx h^{d+1}/t_h$  where  $t_h \equiv t_a(h/a)^z$ .

dimensions of  $k^{(2)}$  are  $x^{d+1}/t$ , as appropriate to a  $(d+1)$ -dimensional bulk problem. For the remainder of this paper we will refer to  $d+1 > z$  and  $d+1 < z$  as the “non-compact” and “compact” cases, respectively.

Consider the long time behavior now. This is completely different to the bulk. In fact at long times the effective dimensionality of the problem changes from  $d+1$  to 1 and, moreover, the reaction kinetics become of *first* order. Let us first investigate the compact case,  $d+1 < z$ . Consider an A particle that was initially within a distance  $l$  of the interface, where  $l \equiv n^{-1/d}$  is the typical separation between reactants. By time  $t_l \equiv t_a(na^d)^{-z/d}$ , its exploration volume will typically contain one B particle, in the other bulk, which was initially within  $l$  of the A particle. Since  $d+1 < z$ , reaction is certain. It follows that for times  $t > t_l$  the interface becomes, in effect, “perfectly absorbing”: almost every reactive species reaching it will suffer a reaction. Thus a density depletion hole develops at the interface (see Fig. 3) and the reaction rate is limited by diffusion to the interface,  $\mathcal{R}_t \approx x_t n$ . One concludes that long time reaction kinetics are now *first* order, with a *first* order rate constant  $k^{(1)}$  given by

$$\dot{\mathcal{R}}_t = k^{(1)} n, \quad k^{(1)} \approx \frac{dx_t}{dt} \sim t^{1/z-1} \quad (t \rightarrow \infty). \quad (5)$$

Notice that the dimensions of  $k^{(1)}$  are  $x/t$ , as would be appropriate to a one-dimensional bulk problem. In correspondence to the kinetics being first order, this DC regime is accompanied by a growing hole of size  $x_t$  in the *one-body* density “correlation function”, *i.e.* in the density field itself,  $n(\mathbf{r})$ . This is very different to the hole, also of size  $x_t$ , which grew in the *two-body* density correlation function for the *second* order  $d+1 < z$  compact DC kinetics at short times, equation (4). For that regime, the density field itself was unchanged from equilibrium.

What are the long time kinetics for the non-compact case,  $d+1 > z$ ? The answer is: the same as for the compact case. The only difference is that the cross over from  $d+1$  to 1-dimensional behavior no longer occurs at  $t_l$ , but at a timescale we name  $t_m^*$ . In this case we can estimate  $t_m^*$  using a mean field picture since the early kinetics are MF. Consider an A particle initially within  $x_t$  of the interface, as in Figure 2. After time  $t$ , it has made  $t/t_a$  “steps”, a fraction  $(h/x_t)$  of which were within the interfacial region where B particles are present at density  $n$ . Thus for each of these interfacial steps the probability that the A particle was in contact with any B particle is  $na^d$ . Hence the total reaction probability,  $P_m$ , is

$$P_m(t) \approx \left( \frac{h}{x_t} \frac{t}{t_a} \right) (na^d) \approx \frac{h}{a} na^d (t/t_a)^{1-1/z} \quad (Q_b = 1/t_a). \quad (6)$$

Setting  $P_m(t_m^*) = 1$ , one obtains  $t_m^*/t_a = [a/(hna^d)]^{z/(z-1)}$ . Thus, for  $t > t_m^*$  any A particle within diffusional range of the interface will definitely have reacted with a B. This is a many-body effect; by  $t_m^*$  any A near the interface is bound to have reacted due to the mean reaction field created by all of the B molecules.

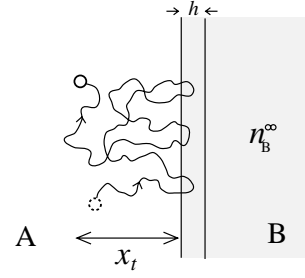


**Fig. 2.** Schematic of the trajectory of an A particle after time  $t$ , given this particle was initially within diffusive range of the interface. Since the number of encounters with the interface is an increasing function of time, even for relatively weakly reactive species the A particle is certain to have reacted at sufficiently long times. The timescale is either  $t_m^*$  or  $t_l$  (see main text).

We conclude that for large times a density depletion hole develops also for the non-compact case, following the same kinetics as equation (5).

So far we have considered “infinitely” reactive species,  $Q_b \approx 1/t_a$ . Such local reactivities  $Q_b$  are realized for radicals [37], and in certain other processes such as phosphorescence quenching [38]. However, these are very exotic exceptions to the general rule: in virtually all practical situations  $Q_b$  is tiny,  $Q_b t_a \lesssim 10^{-6}$ . Indeed, for the vast majority of reacting species,  $Q_b$  values are many orders of magnitude smaller than  $10^{-6}$  [39, 40]. It is essential, therefore, to establish how the picture we have developed above is modified for finitely reactive systems. For non-compact cases,  $d+1 > z$ , there is no qualitative change from the kinetics of equation (4): again, a short time 2nd order MF regime, now with  $k^{(2)} = Q_b h a^d$ , is followed at  $t_m^*$  by a DC first order regime, but now the formula for  $t_m^*$  is modified. Notice that the expression for  $P_m(t)$  in equation (6) is the mean number of collisions experienced by the A particle; multiplying this by the reaction probability per collision,  $Q_b t_a$ , yields the total reaction probability for general  $Q_b$ . Defining  $P_m(t_m^*) \equiv 1$ , we have

$$P_m(t) \approx (Q_b t_a) na^d \left( \frac{t}{t_a} \right)^{1-1/z}, \quad \frac{t_m^*}{t_a} = \left( \frac{1}{Q_b t_a na^d} \right)^{z/(z-1)}, \quad Q \equiv Q_b \frac{h}{a}, \quad (7)$$

where  $Q$  emerges as an *effective* local reaction rate coarse-grained over the interface width  $h$ .

In the compact case,  $d+1 < z$ , kinetics are more fundamentally modified by finite reactivity. For  $Q_b t_a = 1$  we have seen an initial 2nd order DC regime followed at  $t_l$  by 1st order DC kinetics. But for  $Q_b t_a < 1$ , a new MF regime appears at early times. Consider an A–B pair near the interface whose members are initially closer than  $x_t$  to one another, as in Figure 1. By time  $t$ , A has taken  $(t/t_a)(h/x_t)$  steps in the interface. For a fraction  $(a/x_t)^d$  of these, B was in contact with A since B is equally likely to be anywhere within its exploration volume  $x_t^d$ . Thus,

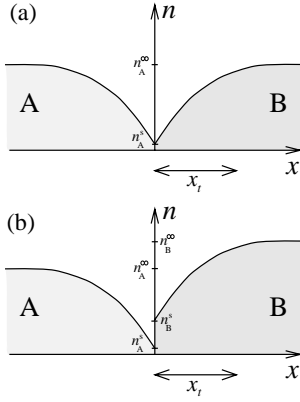


**Fig. 3.** A reactant density depletion hole of size  $x_t \sim t^{1/z}$  grows at the interface for long times. (a) The symmetric case,  $n_A^\infty = n_B^\infty$ . The reactant density at the interface,  $n_A^s$ , tends asymptotically to zero. (b) In the asymmetric case,  $n_B^\infty > n_A^\infty$ , the interfacial density  $n_A^s$  on the dilute side tends to zero, while  $n_B^s$  asymptotes  $n_B^\infty - n_A^\infty$ .

the 2-body reaction probability for this pair is given by

$$P_2(t) \approx \left(\frac{h}{x_t}\right) \left(\frac{a^d}{x_t^d}\right) \left(\frac{t}{t_a}\right) (Q_b t_a) \approx Q t_a \left(\frac{t}{t_a}\right)^{1-(d+1)/z}. \quad (8)$$

This implies a characteristic timescale,  $t_2^*$ , defined such that  $P_2(t_2^*) \equiv 1$ ,

$$t_2^* = t_a \left(\frac{1}{Q t_a}\right)^{z/(z-d-1)}. \quad (9)$$

For  $t > t_2^*$  any pair initially within diffusive range will definitely have reacted; this tells us that kinetics must have 2nd order DC form for such times. Thus the DC regime of equation (4) begins only at  $t_2^*$ ; for shorter times,  $t < t_2^*$ , since  $P_2(t) \ll 1$ , correlations are little disturbed from equilibrium and it follows that MF kinetics apply,  $k^{(2)} = Q_b h a^d$ . In fact, for sufficiently small  $Q$  (“weak systems”)  $t_2^*$  will exceed  $t_m^*$  in which case the 2nd order DC regime will disappear. In later sections we will carefully distinguish between this case and the case of “strong systems” ( $t_2^* < t_m^*$ ).

### Interfacial kinetics: the technical difficulties

In the present work we will develop a near-exact formalism to justify these scaling arguments. The difficulty is the many-body character of this problem. Consider for example the reaction rate per unit area,  $\mathcal{R}_t$ . This equals the number of reactive A–B pairs per unit area which are in contact at the interface,  $\rho_{AB}^s(t)$ , multiplied by the local reactivity  $Q_b$ :

$$\frac{d\mathcal{R}_t}{dt} = \lambda \rho_{AB}^s(t), \quad \lambda \equiv Q_b h a^d = Q a^{d+1} \quad (10)$$

where the quantity  $\lambda$  will turn out to be a natural coupling constant in our theory. Now  $\rho_{AB}^s(t)$  is the two-body

density correlation function  $\rho_{AB}(\mathbf{r}_A, \mathbf{r}_B; t)$  (the number of A–B pairs at  $\mathbf{r}_A, \mathbf{r}_B$  per unit volume squared) evaluated at the interface,  $\mathbf{r}_A = \mathbf{r}_B = 0$ :

$$\rho_{AB}^s(t) \equiv \rho_{AB}(0, 0; t). \quad (11)$$

We take the origin of our coordinate system to lie on the interface plane and we have used translational invariance in the directions parallel to the interface (hence  $\rho_{AB}^s(t)$  is spatially uniform). One sees that to determine the reaction rate we need information on the two-body density correlation function. However, any dynamical equation for the latter inevitably involves three-body correlation functions  $\rho_{ABA}, \rho_{BAB}$ . The dynamics of these objects in turn involve higher order correlations, and so forth. This hierarchical structure is the signature of the many-body nature of the problem.

How can a theory deal with these many-body complexities? One possible approach [23], a mean field approximation, would be to assume  $\rho_{AB}^s(t) = [n^s(t)]^2$ , where  $n^s(t) \equiv n(\mathbf{r} = 0)$  is the density of A (or B) reactants at the interface. This approximation cannot always be valid: for example, in the compact case,  $d + 1 < z$ , this would disagree with the short time 2nd order DC behavior of equation (4) since in this regime the density field is unchanged from equilibrium,  $n^s(t) \approx n(0)$ ; hence the assumption  $\rho_{AB}^s(t) = [n^s(t)]^2$  would wrongly yield  $\mathcal{R}_t \sim t$ . Does this approximation make sense at longer times? Now since we have established (Eq. (5)) the asymptotic law  $\mathcal{R}_t \sim n t^{(1-z)/z}$ , this approximation would then imply  $n^s(t) \sim t^{(1-z)/(2z)}$  which as we will see is correct for the non-compact case only. For the compact case, the long time decay of  $n^s(t)$  is in fact determined by the rate at which fluctuations in the initial distribution of A and B reactants decay. This gives rise to a different decay law, invalidating the local mean field approximation.

To see how densities at the interface,  $n^s(t)$ , decay for large times, consider a simple generalization of the argument of Ovchinnikov and Zeldovich and Toussaint and Wilczek, extended to the interface problem. Consider a region at the interface of volume  $\Omega$ , half of which is on the A side and half on the B side. The difference  $\delta N(t) \equiv N_A(t) - N_B(t)$  between the number of A and B in  $\Omega$  is initially of order  $\sqrt{n\Omega}$ . Now fluctuations in  $\delta N(t)$  can decay by diffusion only. Only if  $\Omega$  is smaller than  $x_t^d$  did these fluctuations have sufficient time to have decayed by time  $t$ . For bigger regions,  $\delta N(t) \approx \delta N(0) \approx \sqrt{n\Omega}$ . Thus reactant densities at the interface, for example, cannot decay faster than  $\sqrt{n x_t^d}/x_t^d \sim \sqrt{n} t^{-d/(2z)}$ . In the compact case,  $d + 1 < z$ , this is a slower decay than  $[\rho_{AB}^s(t)]^{1/2}$ . Thus the local mean field assumption is wrong, and subtle correlations between reactants determine the long time decay. Correspondingly, for the compact case only, there is a segregation of reactants adjacent to the interface into A-rich and B-rich regions of size  $x_t$ .

Various approximation schemes have been used to treat reaction kinetics in the bulk. Typically, the three-body density correlation function is truncated in terms of lower order correlations; this reduces the hierarchy

of reaction-diffusion equations for the many-body correlation functions to a closed set which are solved numerically (see Ref. [41] and references therein). The *ad hoc* nature of such approximations is balanced by their success, as judged from direct numerical simulations [41]. Rigorous analysis was initiated by Doi [42] who developed a general formalism mapping classical many-particle systems onto quantum field theoretic models. Doi's formalism has been the starting point of recent renormalization group approaches to bulk reacting systems [31, 43, 44].

Our approach is rather different to previous ones. We make a small number of simple assumptions which on physical grounds we believe are correct: we assume bounds on certain density correlation functions, and we assume the reaction rate to be a decreasing function of time which is asymptotically a power law. It is possible that these bounds might be proved rigorously, but we do not attempt this here. Having made these assumptions, the subsequent analysis is exact. In the case of systems such as reacting polymers which are not point-like (all the internal polymer degrees of freedom are involved in addition to the locations of the reactive groups) and for which  $z \neq 2$  at small times, our analysis, though not exact, provides a framework for calculating all physically interesting quantities.

The rest of this paper aims to justify the scaling arguments presented above. In Section 2 we present an exact mathematical formulation of the problem. We significantly simplify the problem in Section 3 by postulating bounds on a three-body density correlation function. This allows us to solve for the reaction rate. In Sections 4, 5 and 6 we solve for the reaction rate in the compact, noncompact and marginal ( $z = d + 1$ ) cases. Our results verify the scaling arguments presented above. In Sections 7 and 8 the density profile is calculated, including fluctuation effects and reactant segregation. We conclude with a discussion of our results in Section 9.

## 2 Interfacial pair density, $\rho_{AB}^s$

According to equation (10) the reaction rate is proportional to the density of A–B pairs which are in contact at the interface,  $\rho_{AB}^s(t)$ . In this section, we will obtain an exact self-consistent integral expression for  $\rho_{AB}^s$ .

We consider the general situation, illustrated in Figure 1, where the initial reactant densities  $n_A^\infty, n_B^\infty$  are not necessarily equal. (The entire discussion of Sect. 1 treated the symmetric case  $n_A^\infty = n_B^\infty$  for simplicity.) Our convention will always be that  $n_B^\infty \geq n_A^\infty$ . We choose the  $d$ -dimensional A and B bulk phases to occupy  $x > 0$  and  $x < 0$  respectively, with  $x$  being the direction orthogonal to the interface, and we assume that A and B species have identical dynamics (*i.e.* dynamical exponent  $z$ ).

Throughout this paper, we use the convention that superscript T denotes a  $d$ -dimensional vector lying in the  $(d - 1)$ -dimensional interface. Thus by definition the  $x$ -component of  $\mathbf{r}^T$  vanishes.

Let us begin by treating the case  $z = 2$ , which is then simply generalized to arbitrary  $z$ . The second-quantization representation for classical many-particle

systems developed by Doi [42] and by Zeldovich and Ovchinnikov [45] allows us to derive an exact reaction diffusion equation for the two-body correlation function  $\rho_{AB}(\mathbf{r}_A, \mathbf{r}_B; t)$ . Using Doi's formalism, we show in Appendix A that for small non-interacting Fickian molecules ( $z = 2$ ) with diffusivity  $D$

$$\left\{ \frac{\partial}{\partial t} - D [\nabla_A^2 + \nabla_B^2] \right\} \rho_{AB}(\mathbf{r}_A, \mathbf{r}_B; t) =$$

$$- \lambda \delta(x_A) \delta(\mathbf{r}_A - \mathbf{r}_B) \rho_{AB}(\mathbf{r}_A, \mathbf{r}_B; t)$$

$$- \lambda \delta(x_A) \rho_{ABB}(\mathbf{r}_A, \mathbf{r}_B, \mathbf{r}_A; t)$$

$$- \lambda \delta(x_B) \rho_{ABA}(\mathbf{r}_A, \mathbf{r}_B, \mathbf{r}_B; t), \quad (12)$$

with reflecting boundary conditions at  $x = 0$ . Note the appearance of the coupling constant  $\lambda \equiv Q_b h a^d$  introduced in equation (10). The 3-body correlation function  $\rho_{ABB}(\mathbf{r}_A, \mathbf{r}_B, \mathbf{r}'_B; t)$  is the probability density to find an A–B–B triplet at locations  $\mathbf{r}_A, \mathbf{r}_B, \mathbf{r}'_B$ . A similar definition applies to  $\rho_{ABA}(\mathbf{r}_A, \mathbf{r}_B, \mathbf{r}'_A; t)$ .

The sink terms on the right hand side of equation (12) describe the three ways in which reactions can diminish  $\rho_{AB}(\mathbf{r}_A, \mathbf{r}_B; t)$ . (1) The first *two-body* sink term represents reactions between A–B pairs located at  $\mathbf{r}_A, \mathbf{r}_B$ . The delta functions restrict reactions to  $\mathbf{r}_A, \mathbf{r}_B$  values such that both A and B are in contact (*i.e.* within  $a$  of one another) and both A and B are within the interface of width  $h$  located at  $x = 0$ . These restrictions introduce a factor  $h a^d$ . This is a somewhat coarse-grained description: our “minimal” delta-function sinks are appropriate provided we avoid timescales of order  $t_h \equiv t_a (h/a)^z$  or smaller. (2, 3) The remaining two sink terms in equation (12) describe reactions involving just *one* particle of an A–B pair at  $\mathbf{r}_A, \mathbf{r}_B$ . Such a reaction involves a third particle, weighted by the appropriate 3-body correlation function. These are *many-body* terms; were they absent, one would have a relatively simple closed 2-body system. In the next section we will deal with this difficulty by assuming bounds on the forms of these 3-body correlation functions.

Consider a general value of  $z$  now, for which the two particle free propagator is  $G_t(\mathbf{r}_A, \mathbf{r}'_A; \mathbf{r}_B, \mathbf{r}'_B)$ , namely the probability density an A–B pair is at  $\mathbf{r}_A, \mathbf{r}_B$  at time  $t$  given initial location  $\mathbf{r}'_A, \mathbf{r}'_B$ , in the *absence* of reactions. Without reactions A and B particles are statistically independent; thus  $G_t$  can be written as a product of single particle propagators  $G_t^{(1)}$ :

$$G_t(\mathbf{r}_A, \mathbf{r}'_A; \mathbf{r}_B, \mathbf{r}'_B) = G_t^{(1)}(\mathbf{r}_A, \mathbf{r}'_A) G_t^{(1)}(\mathbf{r}_B, \mathbf{r}'_B). \quad (13)$$

Since  $G_t^{(1)}$  has only one characteristic scale,  $x_t$ , dimensional analysis dictates the scaling form

$$G_t^{(1)}(\mathbf{r}, \mathbf{r}') = \frac{1}{x_t^d} g(\mathbf{r}/x_t, \mathbf{r}'/x_t),$$

$$g(\mathbf{u}, \mathbf{v}) \rightarrow \begin{cases} f(u_x, v_x) & |\mathbf{u} - \mathbf{v}| \ll 1 \\ 0 & |\mathbf{u} - \mathbf{v}| \gg 1 \end{cases} \quad (14)$$

where  $f(u_x, v_x)$  is a function of order unity for every value of its arguments ( $u_x$  and  $v_x$  are the  $x$  components of  $\mathbf{u}, \mathbf{v}$ ,

respectively). The fact that  $f$  depends on  $u_x, v_x$  is a result of the broken translational invariance in the  $x$  direction due to the reflecting boundary at  $x = 0$ .

Returning to equation (12), we can write a self-consistent expression for  $\rho_{AB}(\mathbf{r}_A, \mathbf{r}_B; t)$  in terms of the free propagator  $G_t$ . Setting  $\mathbf{r}_A = \mathbf{r}_B = 0$  one obtains

$$\begin{aligned} \rho_{AB}^s(t) &= n_A^\infty n_B^\infty - \lambda \int_0^t dt' S^{(d+1)}(t-t') \rho_{AB}^s(t') \\ &\quad - \lambda [I_m^A(t) + I_m^B(t)], \end{aligned} \quad (15)$$

where

$$S^{(d+1)}(t) \equiv \int d\mathbf{r}^{T'} G_t(0, \mathbf{r}^{T'}; 0, \mathbf{r}^{T'}) \approx \frac{1}{x_t^{d+1}} \quad (16)$$

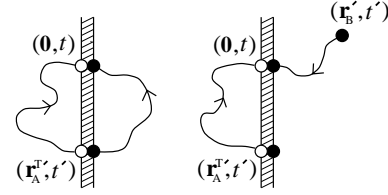
is the two-body ‘‘return probability’’, namely the probability density an A–B pair is in contact at time  $t$  at the interface, given it was in contact somewhere within the interface at  $t = 0$ . We have used equation (14) to show that  $S^{(d+1)}(t) \approx 1/x_t^{d+1}$  has the same scaling form as the return probability in a  $(d+1)$ -dimensional bulk problem. In equation (15), the two-body integral involving  $S^{(d+1)}(t)$  represents depletion in the interfacial reactive pair density  $\rho_{AB}^s(t)$  due to A–B pairs whose members reacted with one another at times  $t' < t$  and therefore failed to reach the origin at  $t$  (see Fig. 4). The terms  $I_m^A(t), I_m^B(t)$  measure depletion due to many-body effects:

$$\begin{aligned} I_m^A(t) &\equiv \int_0^t dt' \int d\mathbf{r}_A^{T'} d\mathbf{r}_B^{T'} G_{t-t'}(0, \mathbf{r}_A^{T'}; 0, \mathbf{r}_B^{T'}) \\ &\quad \times \rho_{ABB}(\mathbf{r}_A^{T'}, \mathbf{r}_B^{T'}, \mathbf{r}_A^{T'}; t'), \\ I_m^B(t) &\equiv \int_0^t dt' \int d\mathbf{r}_A^{T'} d\mathbf{r}_B^{T'} G_{t-t'}(0, \mathbf{r}_A^{T'}; 0, \mathbf{r}_B^{T'}) \\ &\quad \times \rho_{ABA}(\mathbf{r}_A^{T'}, \mathbf{r}_B^{T'}, \mathbf{r}_B^{T'}; t'). \end{aligned} \quad (17)$$

These integrals subtract off any A–B pair only one member of which was involved in a reaction an earlier time (see Fig. 4).

We will see later that the two-body integral involving  $S^{(d+1)}(t)$  in equation (15) is important at short times; for such times reaction kinetics are hence like those in a  $(d+1)$ -dimensional bulk reaction problem. At longer times the many-body terms  $I_m^A(t), I_m^B(t)$  are always dominant and kinetics cross over to one-dimensional form.

Equations (15–17) are immediately generalized to arbitrary dynamics with arbitrary values of  $z$ : one simply replaces the Gaussian ( $z = 2$ ) propagator  $G_t$ , describing Fickian diffusion, with the appropriate propagator describing the dynamics. Now this would be a true statement for the abstract concept of small (*i.e.* point-like) molecules obeying  $x_t \sim t^{1/z}$  with  $z \neq 2$ . However, in practice non-Fickian diffusion normally results from the small reactive species belonging to a large structure with complex internal dynamics. The most important case is when the reactive group is a single monomer unit belonging to a polymer chain of  $N$  units. In these cases the dynamics



two-body term    many-body term

**Fig. 4.** The depletion in the number density of reactive A–B pairs at the origin from the value it would have in the absence of reactions originates from three terms, equation (15). The two-body term counts those A–B pairs which would have been at the origin at time  $t$ , but failed to arrive because *both* members reacted at an earlier time  $t'$  at point  $\mathbf{r}_A^{T'}$ . The first many-body term ( $I_m^A(t)$ , described in the figure) counts A–B pairs which would have been at the origin had there been no reactions, but failed to arrive because *one* member of the pair, the A member, reacted at an earlier time. The second many body term,  $I_m^B(t)$ , is identical except the roles of A and B are interchanged.

of equation (15) are not exact because they incorrectly presuppose a closed relationship in terms of the degrees of freedom specifying the location of the reactive species only. A proper treatment must first average out the other degrees of freedom (*e.g.* the locations of the other  $N-1$  monomers in the polymer case); this is non-trivial and requires renormalization group (RG) methods [46]. However, RG studies of 2-body bulk polymer reaction kinetics [36, 46] indicate that the basic physics is completely captured by the approximate closing of the system in terms of these coordinates only: correct scaling behaviors are obtained, only the prefactors being unreliable. These issues are discussed in detail in references [36, 46, 47]. Therefore for the remainder of this paper we assume the validity of equations (15–17) for any value of  $z$ .

### 3 Structure of many-body integral terms $I_m^A(t), I_m^B(t)$

In Section 2 we derived a self-consistent solution for the interfacial reactive pair density  $\rho_{AB}^s(t)$ , equation (15). Unfortunately this is not in a closed form for  $\rho_{AB}^s(t)$ , since the many-body terms involve higher order correlation functions. In this section we introduce our three simple, physically motivated assumptions. These enable us to express  $I_m^A(t), I_m^B(t)$  in terms of  $\rho_{AB}^s(t)$ , which in the following section will allow us to obtain a closed solution for  $\rho_{AB}^s$ . Most calculational details will be left for Appendix B.

Consider the three-body correlation function  $\rho_{ABB}$  appearing in  $I_m^A(t)$  of equation (17). Let us introduce the conditional density of B particles at  $\mathbf{r}_B$  given an A–B pair at the origin,

$$\rho_{BAB}(\mathbf{r}_B|0, 0; t) \equiv \frac{\rho_{ABB}(0, \mathbf{r}_B, 0; t)}{\rho_{AB}^s(t)}. \quad (18)$$

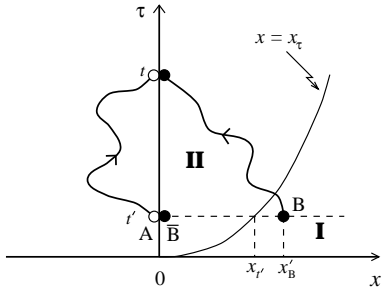


**Fig. 5.** Trajectories of a typical A–B pair which at time  $t$  is at the origin, and whose A member reacted at the interface at time  $t'$  with another B-type particle ( $\bar{B}$ ). Trajectories are shown projected onto the  $x$ – $\tau$  plane where  $x$  is distance from the interface and  $\tau$  is time. The properties of trajectories of this type determine the value of the integration which determines the many body term  $I_m^A(t)$  (see Eq. (19) and following discussion in main text). At  $t'$ , the B particle of the pair has  $x$ -coordinate  $x'_B$  which can be (a) in region I, if  $x'_B > x_{t'}$  (as shown in the figure), or (b) in region II, if  $x'_B < x_{t'}$ .

Noting that translational invariance parallel to the interface plane allows the replacement  $\rho_{ABB}(\mathbf{r}_A^{T'}, \mathbf{r}'_B, \mathbf{r}_A^{T'}; t') \rightarrow \rho_{ABB}(0, \mathbf{r}'_B - \mathbf{r}_A^{T'}, 0; t')$ , we can express  $I_m^A(t)$  as

$$I_m^A(t) = \int_0^t dt' \int d\mathbf{r}'_B F_{t-t'}(\mathbf{r}'_B) \rho_{BAB}(\mathbf{r}'_B|0, 0; t') \rho_{AB}^s(t'),$$

$$F_{t-t'}(\mathbf{r}'_B) \equiv \int d\mathbf{r}_A^{T'} G_{t-t'}(0, \mathbf{r}_A^{T'}; 0, \mathbf{r}'_B + \mathbf{r}_A^{T'}). \quad (19)$$

In Figure 5 we identify two physically distinct space-time regions which contribute to  $I_m^A(t)$  in the  $\mathbf{r}'_B, t'$  integration of equation (19). The assumptions we are about to introduce are based on the following expectations about the behavior of the conditional 3-body density in these two regions. In region I, defined by points with  $x$ -coordinate  $x'_B > x_{t'}$ , the conditional density at time  $t'$  approximates its far field value,  $\rho_{BAB}(\mathbf{r}'_B|0, 0; t') \approx n_B^\infty$ . This is because far into region I such locations  $\mathbf{r}'_B$  are beyond diffusional range of the interface: hence density correlations at  $\mathbf{r}'_B$  cannot have been influenced by reaction events during  $(0, t')$ . On the other hand, in region II ( $x'_B < x_{t'}$ ), this conditional density will be strongly influenced by such reaction events. Whatever this density field may be, we expect that its maximum will never be greater than a value of the order of  $n_B^\infty$ . Reactions tend to reduce densities, but we do not exclude the possibility that subtle B–A–B correlations could locally elevate the field somewhat.

Let us now translate the above general physical expectations into two specific assumptions on the conditional density field. Simultaneously we introduce a third assumption, concerning  $\rho_{AB}^s(t)$ .

#### Assumption 1

There exists a positive finite constant  $U$ , such that:

$$\frac{\rho_{BAB}(\mathbf{r}'_B|0, 0; t')}{n_B^\infty} \leq U. \quad (20)$$

This amounts to assuming that irrespective of what reaction-induced correlations exist between points 0 and  $\mathbf{r}'_B$ , the conditional density of B particles at  $\mathbf{r}'_B$  will always be less than, or at most of the order of, the far-field density of B reactants in the B bulk.

#### Assumption 2

There exists a positive finite constant  $L$ , such that:

$$\frac{\rho_{BAB}(\mathbf{r}'_B|0, 0; t')}{n_B^\infty} \geq L, \quad \text{for } \frac{x'_B}{x_{t'}} > 1. \quad (21)$$

Roughly speaking this amounts to assuming that points in region I are uncorrelated with the interface.

#### Assumption 3

$\rho_{AB}^s(t)$  is a decreasing function of time which is asymptotically a power law.

Assumptions 1 and 2 immediately imply the same two assumptions but with A and B interchanged (since A and B are arbitrarily chosen labels). That is, the field  $\rho_{ABA}(\mathbf{r}'_A|0, 0; t')$  appearing in  $I_m^B(t)$  obeys two assumptions analogous to 1 and 2.

Based on these assumptions, we show in Appendix B that the contribution to  $I_m^A(t)$  from integration over region I is a fraction of order unity of the value of  $I_m^A(t)$ . (Equivalently, a fraction of order unity of the A–B interface pairs which involve one previously reacted A and are subtracted off by  $\lambda I_m^A(t)$ , involve a B member originating from region I.) Therefore, since assumptions 1 and 2 imply that  $\rho_{BAB}$  equals  $n_B^\infty$  in region I to within a finite prefactor bounded above and below, it follows that if we replace  $\rho_{BAB}(\mathbf{r}'_B|0, 0; t') \rightarrow n_B^\infty$  in the integrand of  $I_m^A(t)$  in equation (19), the result will equal the actual value of  $I_m^A(t)$  to within a (time-dependent) prefactor of order unity,  $\alpha(t)$ . Making this replacement, using equation (13), and performing an analogous replacement for  $I_m^B(t)$ , one obtains

$$I_m^A(t) = \alpha(t) n_B^\infty \int_0^t dt' S^{(1)}(t-t') \rho_{AB}^s(t'),$$

$$I_m^B(t) = \beta(t) n_A^\infty \int_0^t dt' S^{(1)}(t-t') \rho_{AB}^s(t'), \quad (22)$$

where  $\alpha(t), \beta(t)$ , are bounded positive functions of order unity,

$$\alpha_{\min} \leq \alpha(t) \leq \alpha_{\max},$$

$$\beta_{\min} \leq \beta(t) \leq \beta_{\max}. \quad (23)$$

Here  $\alpha_{\min}, \alpha_{\max}, \beta_{\min}, \beta_{\max}$  are finite positive constants. The one-dimensional return probability  $S^{(1)}(t)$  is defined as

$$S^{(1)}(t) \equiv \int d\mathbf{r}_A^{T'} G_t^{(1)}(0, \mathbf{r}_A^{T'}) \approx \frac{1}{x_t}. \quad (24)$$

It measures the probability a reactant initially at the interface returns to the interface after time  $t$ . The scaling form,  $S^{(1)} \sim 1/x_t$ , is easily derived from the scaling form of the propagator  $G_t^{(1)}$ , equation (14).

#### 4 Reaction rate in compact case ( $d + 1 < z$ )

Having expressed the many-body terms  $I_m^A(t), I_m^B(t)$  in terms of the interfacial reactive pair density  $\rho_{AB}^s(t)$ , we can solve for the reaction rate per unit area  $\dot{\mathcal{R}}_t = \lambda \rho_{AB}^s(t)$ . According to the results of the previous section, equation (22), the self-consistent solution for  $\rho_{AB}^s(t)$ , equation (15), can be written

$$\begin{aligned} \rho_{AB}^s(t) &= n_A^\infty n_B^\infty - \lambda \int_0^t dt' S^{(d+1)}(t-t') \rho_{AB}^s(t') \\ &\quad - \lambda n(t) \int_0^t dt' S^{(1)}(t-t') \rho_{AB}^s(t'), \\ n(t) &\equiv \alpha(t) n_B^\infty + \beta(t) n_A^\infty. \end{aligned} \quad (25)$$

This ‘‘solution’’ of course involves the unknown function  $n(t)$ . From the arguments of the previous section following from our assumptions 1 and 2, we know that  $n(t)$  is bounded above and below. Now according to assumption 3, asymptotically  $\rho_{AB}^s(t) \sim t^{-\delta}$  with  $\delta > 0$ . Substituting this power law in equation (25), and substituting  $x_t \sim t^{1/z}$  in the scaling forms of  $S^{(d+1)}(t)$  and  $S^{(1)}(t)$  from equations (16, 24), one finds that as  $t \rightarrow \infty$  the many-body term dominates over the other time-dependent terms in equation (25), and up to a constant prefactor is equal to  $n(t)t^{1-1/z-\delta}$ . It follows that at long enough times the many-body term must equal the first term on the rhs of equation (25),  $n_A^\infty n_B^\infty$ , plus higher order corrections. Since  $n(t)$  is bounded, this implies that  $\delta = 1 - 1/z$  and that  $n(t)$  tends to a constant at long times,  $n(\infty)$ . We will prove in Section 7 that this constant is none other than the reactant density in the more *dense* of the two phases:

$$n(\infty) = n_B^\infty. \quad (26)$$

We remind the reader of our convention throughout this study,  $n_B^\infty \geq n_A^\infty$ .

Laplace transforming equation (25),  $t \rightarrow E$ , and recalling that  $\dot{\mathcal{R}}_t = \lambda \rho_{AB}^s(t)$ , it is simple to obtain the following self-consistent relation for the Laplace transform of the reaction rate per unit area,  $\dot{\mathcal{R}}_t(E)$ :

$$\begin{aligned} \dot{\mathcal{R}}_t(E) &= \frac{\lambda n_A^\infty n_B^\infty}{E [1 + \lambda S^{(d+1)}(E) + \lambda n_B^\infty \gamma(E) S^{(1)}(E)]}, \\ \gamma(E) &\equiv \frac{n(E) * [S^{(1)}(E) \dot{\mathcal{R}}_t(E)]}{n_B^\infty S^{(1)}(E) \dot{\mathcal{R}}_t(E)}. \end{aligned} \quad (27)$$

Here, \* indicates convolution in Laplace space. The function  $\gamma(E)$  has a simple form for small  $E$ ; since, by virtue of equation (26),  $n(E \rightarrow 0) = n_B^\infty/E$ , then from equation (27) one has

$$\gamma(E) = 1 + O(E) \quad (E \rightarrow 0). \quad (28)$$

Now from equations (1, 16, 24),  $S^{(d+1)}(t)$  and  $S^{(1)}(t)$  are algebraic in time. Their Laplace transforms have the form  $S^{(d+1)}(E) \sim E^{(d+1)/z-1}$  (valid only in compact dimensions,  $d + 1 < z$ ) and  $S^{(1)}(E) \sim E^{1/z-1}$  (always valid).

This section is concerned with the compact case; then we can rewrite  $\dot{\mathcal{R}}_t(E)$  in two ways:

$$\begin{aligned} \dot{\mathcal{R}}_t(E) &\approx \frac{\lambda n_A^\infty n_B^\infty}{E \{1 + (Et_2^*)^{[(d+1)/z]-1} + \gamma(E)(Et_m^*)^{(1/z)-1}\}} \\ &\approx \frac{\lambda n_A^\infty n_B^\infty}{E \{1 + (Et_2^*)^{[(d+1)/z]-1} [1 + \gamma(E)(Et_l)^{-d/z}]\}}, \end{aligned} \quad (29)$$

where

$$\begin{aligned} t_l &\equiv t_a \left( \frac{1}{n_B^\infty a^d} \right)^{z/d}, \\ t_m^* &\equiv t_a \left( \frac{1}{Qt_a n_B^\infty a^d} \right)^{z/(z-1)}, \\ t_2^* &\equiv t_a \left( \frac{1}{Qt_a} \right)^{z/[z-(d+1)]}, \end{aligned} \quad (30)$$

are essentially the three naturally occurring timescales introduced in Section 1, generalized to the case of unequal initial reactant densities ( $n_B^\infty \geq n_A^\infty$ ). It is important to note that the characteristic density determining these timescales is that of the *denser* bulk phase B. In equation (29) for simplicity we have neglected numerical prefactors in the terms in the denominator.

Note that the three characteristic timescales obey

$$t_m^* = (t_2^*)^{1-d/(z-1)} (t_l)^{d/(z-1)} \quad (31)$$

which implies that the magnitude of  $t_m^*$  always lies between those of  $t_2^*$  and  $t_l$ . Hence there are only 2 cases (see Fig. 6). (a) For strongly reactive (‘‘strong’’) systems,  $Q > Q^*$ , the ordering of timescales is  $t_2^* < t_m^* < t_l$ . (b) For ‘‘weak’’ systems,  $Q < Q^*$ , one has  $t_l < t_m^* < t_2^*$ . The boundary between strong and weak regimes is defined by a critical effective local reactivity, at which  $t_2^* = t_m^* = t_l$ :

$$Q^* t_a \equiv (n_B^\infty a^d)^{[z-(d+1)]/d}. \quad (32)$$

#### 4.1 Strong systems: $Q > Q^*$ , $t_2^* < t_m^* < t_l$

Before evaluating  $\dot{\mathcal{R}}_t$  in different time regimes, we note that the many body term (the third term in the denominator in Eq. (29)) is unimportant whenever  $Et_l \gg 1$  (corresponding to  $t \ll t_l$ ). Consider the term (that involving  $S^{(1)}$ ) in equation (25) from which this many body contribution is derived. Now imagine replacing  $n(t)$  in this term by its maximum value,  $n(t) \rightarrow n_{\max} \equiv \alpha_{\max} n_B^\infty + \beta_{\max} n_A^\infty$ , such that  $n(E) = n_{\max}/E$  and hence  $\gamma(E) = n_{\max}/n(\infty) \approx 1$ . It would then indeed follow that the many body term in equation (29) is higher order for  $Et_l \gg 1$ . Clearly, then, this must always be true.

Consider firstly short times,  $E^{-1} \ll t_l$ . The many body term can then be neglected. Considering the two cases  $E^{-1} \ll t_2^*$  and  $t_2^* \ll E^{-1} \ll t_l$ , respectively, inverse

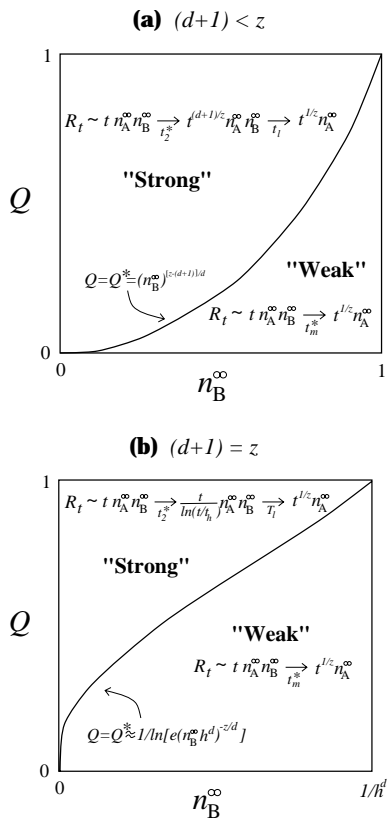


**Fig. 6.** Reaction rate per unit area as a function of time in the  $Q$ - $n_B^\infty$  plane ( $n_B^\infty \geq n_A^\infty$ ). Units are chosen such that  $a = t_a = 1$ . (a) Compact case ( $d+1 < z$ ). (b) Marginal case ( $d+1 = z$ ). Reaction kinetics in the noncompact case are the same as in the “weak” regions of (a) and (b).

Laplace transformation of equation (29) yields

$$\begin{aligned} \dot{\mathcal{R}}_t &= k^{(2)} n_A^\infty n_B^\infty, \\ k^{(2)} &\approx \begin{cases} \lambda & t \ll t_2^* \\ dx_t^{d+1}/dt \sim t^{(d+1)/z-1} & t_2^* \ll t \ll t_l \end{cases}. \end{aligned} \quad (33)$$

These are 2nd order rate kinetics. An initial MF regime is followed at  $t_2^*$  by a DC regime. Notice that the timescale  $t_m^*$  is irrelevant. We remind the reader that our analysis does not describe times less than  $t_h$  (see comments following Eq. (12)); hence, if  $Q$  is so great that equation (30) implies  $t_2^* < t_h$ , then equation (33) correctly describes the second DC regime only.

Now consider very long times  $E^{-1} \gg t_l$ ; the many-body term in equation (29) is then dominant. Since at long enough times we may replace  $\gamma(E) \rightarrow 1$  as discussed, one now finds *first* order kinetics:

$$\dot{\mathcal{R}}_t = k^{(1)} n_A^\infty, \quad k^{(1)} \approx \frac{dx_t}{dt} \sim t^{1/z-1} \quad (t \gg t_l). \quad (34)$$

Thus, at long enough times the reaction rate is controlled by the diffusion to the interface of the more *dilute* A species.

## 4.2 Weak systems: $Q < Q^*$ , $t_l < t_m^* < t_2^*$

Now the many-body term in the curly brackets in equation (29) is much smaller than 1 whenever  $E^{-1} \ll t_m^*$  (this can be seen by replacing  $n(t)$  with its maximum value as in Sect. 4.1). But for such  $E$  values, it is automatically true that  $Et_2^* \ll 1$  by virtue of the definition of weak systems ( $t_2^* > t_m^*$ ), and hence the 2-body term in equation (29) is also much smaller than unity. It follows that MF 2nd order kinetics pertain for all times less than  $t_m^*$

$$\dot{\mathcal{R}}_t = k^{(2)} n_A^\infty n_B^\infty, \quad k^{(2)} \approx \lambda \quad (t \ll t_m^*). \quad (35)$$

Notice that the 2-body and many-body terms are both proportional to negative powers of  $E$ , and that the magnitude of the many-body term’s exponent is the greatest of the two. Now consider  $E^{-1} \gg t_m^*$ , when the many body term is much bigger than unity. It follows that this term is then also much bigger than the 2-body term, because  $t_m^* < t_2^*$  for these weak cases. Thus kinetics are first-order for  $t \gg t_m^*$ :

$$\dot{\mathcal{R}}_t = k^{(1)} n_A^\infty, \quad k^{(1)} \approx \frac{dx_t}{dt} \sim t^{1/z-1} \quad (t \gg t_m^*). \quad (36)$$

To obtain equation (36) we have replaced  $\gamma(E) \rightarrow 1$  for small  $E$ . For weak systems, neither  $t_2^*$  nor  $t_l$  are relevant. The reactivity is so small that the two-body term is never relevant, and 2nd order DC kinetics are absent.

## 5 Reaction rate in marginal case ( $d+1 = z$ )

The previous section dealt with low compact dimensions, for which the 2-body return probability in Laplace space had the form  $S^{(d+1)}(E) \sim E^{(d+1)/z-1}$ . For  $d+1 \geq z$ , this is no longer true. In this section we consider the marginal case,  $d+1 = z$ ; thus  $S^{(d+1)} \approx 1/x_t^{d+1} \sim 1/t$ , giving

$$\begin{aligned} S^{(d+1)}(E) &\approx \int_{t_h}^{\infty} dt e^{-Et} \frac{t_h}{h^{d+1} t} \\ &\approx \frac{t_h}{h^{d+1}} \ln[1/Et_h] \quad (Et_h \ll 1). \end{aligned} \quad (37)$$

We have introduced a cut-off at  $t = t_h$ ; at shorter times  $S^{(d+1)}(t)$  crosses over to a form appropriate to a  $d$ -dimensional bulk problem,  $S^{(d+1)} \approx 1/(hx_t^d)$  whose time integral gives a contribution of the same order as that from the lower limit in equation (37).

Aside from this modification, all steps leading to equation (29) of the compact case are unchanged: the expression for the reaction rate  $\dot{\mathcal{R}}_t(E)$  (Eq. (27)) remains valid, and the form of  $S^{(1)}(E)$  is unchanged. Thus,

$$\begin{aligned} \dot{\mathcal{R}}_t(E) &\approx \frac{\lambda n_A^\infty n_B^\infty}{E \left\{ 1 + \frac{\ln(1/Et_h)}{\ln(et_2^*/t_h)} + \gamma(E)(Et_m^*)^{1/z-1} \right\}} \\ &\approx \frac{\lambda n_A^\infty n_B^\infty}{E \left\{ 1 + \frac{\ln(1/Et_h)}{\ln(et_2^*/t_h)} \left[ 1 + \gamma(E) \frac{(Et_l)^{-d/z}}{\ln(1/Et_h)} \right] \right\}}. \end{aligned} \quad (38)$$

Here the definitions of  $t_l$  and  $t_m^*$  are unchanged from the compact case (Eq. (30)), but now

$$t_2^* \equiv (t_h/e) e^{1/(Qt_a)}. \quad (39)$$

Let us define  $T_l$  to be the time such that for  $E < T_l^{-1}$  the many-body term ( $\propto S^{(1)}(E)$ ) dominates over the two-body term ( $\propto S^{(d+1)}(E)$ ) in the denominator of equation (38):

$$\frac{T_l}{t_l} = [\ln(eT_l/t_h)]^{z/d}. \quad (40)$$

(We have included factors of  $e$  in the definitions of  $t_2^*$  and  $T_l$  above simply to ensure continuity of reaction rates; see Eqs. (42, 43) below.)

Analogously to the compact case, the condition  $t_2^* = t_m^* = T_l$  defines a critical reactive strength  $Q^*$ ,

$$Q^* t_a \equiv \frac{1}{\ln[eT_l/t_h]}, \quad (41)$$

defining the boundary between “weak” and “strong” kinetics (see Fig. 6), for which it can be shown that the 3 relevant timescales have the same orderings as for the compact case.

### 5.1 Strong systems: $Q > Q^*$ , $t_2^* < t_m^* < T_l$

Consider first short times,  $E^{-1} \ll T_l$ . Similar reasoning as for the compact cases implies that the many-body term in equation (38) can be neglected for such  $E$  values. Considering the two cases  $E^{-1} \ll t_2^*$  and  $E^{-1} \gg t_2^*$  one obtains

$$\begin{aligned} \dot{\mathcal{R}}_t &= k^{(2)} n_A^\infty n_B^\infty, \\ k^{(2)} &\approx \begin{cases} \lambda & t \ll t_2^* \\ h^{d+1}/[t_h \ln(et/t_h)] & t_2^* \ll t \ll T_l \end{cases}. \end{aligned} \quad (42)$$

The logarithm arises after inverse Laplace transformation of  $1/\{E \ln(1/Et_h)\}$  which gives  $1/\ln(t/t_h)$  for  $t \gg t_h$ . This is shown in Appendix C.

For long times,  $E^{-1} \gg T_l$ , the many-body term dominates. Using  $\gamma(E) \approx 1$  for small enough  $E$ , which is easily demonstrated using similar arguments to those for the compact case, one finds first-order DC kinetics which are no different in structure to those for the compact case (see Eqs. (34, 36)):

$$\begin{aligned} \dot{\mathcal{R}}_t &= k^{(1)} n_A^\infty, \\ k^{(1)} &\approx \frac{dx_t}{dt} \sim t^{1/z-1} \quad (t \gg T_l). \end{aligned} \quad (43)$$

### 5.2 Weak systems: $Q < Q^*$ , $T_l < t_m^* < t_2^*$

For small times,  $E^{-1} \ll t_m^*$ , the many body term is much less than unity; this is also true of the 2-body term since  $t_2^* > t_m^*$  (definition of weak system). On the other hand,

when  $E^{-1} \gg t_m^*$ , the many body term is much larger than unity; it is also much bigger than the logarithmic 2-body term since  $E^{-1} \gg T_l$  follows automatically, because  $T_l < t_m^*$ . Thus

$$\dot{\mathcal{R}}_t = \begin{cases} k^{(2)} n_A^\infty n_B^\infty, & k^{(2)} \approx \lambda & (t \ll t_m^*) \\ k^{(1)} n_A^\infty, & k^{(1)} \approx dx_t/dt \sim t^{1/z-1} & (t \gg t_m^*) \end{cases}. \quad (44)$$

## 6 Reaction rate in noncompact case ( $d + 1 > z$ )

In this section high non-compact dimensions are considered,  $d + 1 > z$ . Perhaps the commonest physical example of small molecules ( $z = 2, d = 3$ ) belongs to this class. Mathematically, the only distinguishing feature is that the Laplace transform of the 2-body return probability is now dominated by small times, since  $S^{(d+1)}(t)$  of equation (16) now decays faster than  $1/t$  for times  $t > t_h$ :

$$S^{(d+1)}(E) \approx \int_{t_h}^{\infty} dt e^{-Et} \frac{1}{h^{d+1}} \left(\frac{t_h}{t}\right)^{(d+1)/z} \approx \frac{t_h}{h^{d+1}} \quad (Et_h \ll 1, z < d + 1 < z + 1). \quad (45)$$

The above result is determined by the dominant cut-off at  $t = t_h$ . In fact it is valid only provided  $d < z$  because only then is the  $t < t_h$  time integral dominated by its upper limit,  $t = t_h$ : for these smallest times (which have been neglected in the original statement of our model, Eq. (12)) one has in effect an infinite *bulk* reaction problem. It is as if the interface were infinitely large. Correspondingly, the true return probability is  $S^{(d+1)} \approx 1/(hx_t^d)$  for  $t < t_h$ . When time integrated, for dimensions so high that even bulk reaction kinetics are non-compact,  $d > z$ , the lower cut-off at  $t_a$  is now dominant,  $\int_{t_a}^{t_h} e^{-Et} S^{(d+1)} dt \approx t_a S^{(d+1)}(t_a)$  for  $Et_h \ll 1$ . This contribution now exceeds that displayed in equation (45), and one has

$$S^{(d+1)}(E) \approx \frac{t_a}{ha^d} \quad (Et_h \ll 1, d > z). \quad (46)$$

Consider firstly  $z < d + 1 < z + 1$ . The reaction rate in Laplace space of equation (27) now reads

$$\dot{\mathcal{R}}_t(E) \approx \frac{\lambda n_A^\infty n_B^\infty}{E \{1 + Q_b t_a (a^d t_h / h^d t_a) + \gamma(E) (Et_m^*)^{1/z-1}\}}. \quad (47)$$

Here  $\gamma(E)$  is the quantity defined in equation (27) and, as for the compact and marginal cases, it can be shown that  $\gamma(E) \approx 1$  for small enough  $E$ . Thus for  $Q_b t_a < (a/h)^{z-d}$

$$\dot{\mathcal{R}}_t = \begin{cases} k^{(2)} n_A^\infty n_B^\infty, & k^{(2)} \approx \lambda & (t \ll t_m^*) \\ k^{(1)} n_A^\infty, & k^{(1)} \approx dx_t/dt \sim t^{1/z-1} & (t \gg t_m^*) \end{cases} \quad (48)$$

whilst for  $Q_b t_a > (a/h)^{z-d}$  one has

$$\dot{\mathcal{R}}_t = \begin{cases} k^{(2)} n_A^\infty n_B^\infty, & k^{(2)} \approx h^{d+1}/t_h \\ & (t \ll t_h (n_B^\infty h^d)^{z/(1-z)}) \\ k^{(1)} n_A^\infty, & k^{(1)} \approx dx_t/dt \sim t^{1/z-1} \\ & (t \gg t_h (n_B^\infty h^d)^{z/(1-z)}) \end{cases}. \quad (49)$$

Now consider the highest dimensions,  $d > z$ . Then  $\dot{\mathcal{R}}_t(E)$  is as in equation (47), except one replaces  $Q_b t_a (a^d t_h / h^d t_a) \rightarrow Q_b t_a$ . This leads to equation (48) which is now valid for all  $Q_b$  values.

## 7 Density profile

We have seen that short time 2nd order reaction kinetics cross over at a regime-dependent timescale to 1st order diffusion-controlled kinetics. This suggests that the density fields on either side of the interface,  $n_A(\mathbf{r}_A; t)$ ,  $n_B(\mathbf{r}_B; t)$ , are uniform for shorter times but develop depletion holes at the interface of size  $x_t$  when the 1st order kinetics onset. To demonstrate this explicitly, we begin by using Doi's formalism in Appendix A to derive the density field dynamics for small molecules ( $z = 2$ ). We will then generalize results to arbitrary dynamical exponent  $z$ . For  $z = 2$ , we find

$$\begin{cases} \left\{ \frac{\partial}{\partial t} - D \nabla_A^2 \right\} n_A(\mathbf{r}_A; t) = -\lambda \delta(x_A) \rho_{AB}^s(t), \\ \left\{ \frac{\partial}{\partial t} - D \nabla_B^2 \right\} n_B(\mathbf{r}_B; t) = -\lambda \delta(x_B) \rho_{AB}^s(t). \end{cases} \quad (50)$$

The sink terms on the right hand sides of equation (50) are proportional to the number of A-B pairs which are in contact at the interface, per unit area. Noting that translational invariance parallel to the interface plane implies  $n_A, n_B$  depend on  $x_A$  and  $x_B$  only, equation (50) has solution

$$\begin{aligned} n_A(x_A; t) &= n_A^\infty - \lambda \int_0^t dt' G_{t-t'}^{(1)}(x_A) \rho_{AB}^s(t'), \\ n_B(x_B; t) &= n_B^\infty - \lambda \int_0^t dt' G_{t-t'}^{(1)}(x_B) \rho_{AB}^s(t'), \end{aligned} \quad (51)$$

where  $G_t^{(1)}(x) \equiv \int d\mathbf{r}^T G_t^{(1)}(\mathbf{r}, 0)$  is the weighting for a particle, initially at the interface, to be distant  $x$  from the interface after time  $t$ . For arbitrary  $z$ , one just uses the appropriate propagator  $G_t$  in equation (51).

Before proceeding, let us use the above dynamics to prove equation (10),  $\dot{\mathcal{R}}_t = \lambda \rho_{AB}^s(t)$ , a result that we have so far assumed as physically obvious. Now the total number of reactions per unit area is  $\mathcal{R}_t = \int dx_A [n_A^\infty - n_A(x_A; t)]$ ; integrating the first of equations (51) over all  $x_A$  and using the fact that  $G_t^{(1)}(x)$  is normalized to unity, one has  $\mathcal{R}_t = \lambda \int_0^t dt' \rho_{AB}^s(t')$  which proves the desired result.

In the below we need calculate only one of the density fields, say the less dense field  $n_A$ , since one field uniquely

implies the other. This follows after subtracting the two equations in (51), and using  $G_t^{(1)}(x) = G_t^{(1)}(-x)$ , giving

$$n_A(x; t) - n_B(-x; t) = n_A^\infty - n_B^\infty. \quad (52)$$

That is, the difference between mean A and B reactant densities at equal distances from the interface is constant in time.

### 7.1 Long time density at interface

It may appear that equation (51) together with equations (10, 27) provide a closed solution for the density fields. However, in fact equation (27) involves the unknown function  $\gamma(E)$ , whose small  $E$  behavior is needed to obtain the long time density fields. Hitherto we have asserted that its asymptotic behavior is  $\gamma(0) = 1$ , equivalent to the assertion that  $n(\infty) = n_B^\infty$  (see Eqs. (26-28) and surrounding discussions). We must now prove these assertions. To do so, we will first argue that the A density at the interface,  $n_A^s(t) \equiv n_A(0; t)$ , vanishes for long times. This extra piece of information will allow the determination of  $\gamma(0)$ .

We are able to prove  $n_A^s(\infty) = 0$  by first relating  $n_A^s$  to the like particle correlation functions,  $\rho_{AA}^s(t) \equiv \rho_{AA}(0, 0; t)$  and  $\rho_{BB}^s(t) \equiv \rho_{BB}(0, 0; t)$ , on the strength of the following physically motivated assumption on these functions:

**Assumption 4**

$$[n_A^s(t)]^2 \leq \rho_{AA}^s(t), \quad [n_B^s(t)]^2 \leq \rho_{BB}^s(t). \quad (53)$$

This states that reaction-induced correlations can only increase density-density correlations of like particles, relative to the totally random case where one would have  $\rho_{AA}^s(t) = [n_A^s(t)]^2$ . That is, we admit the possibility of clustering of like particles.

To obtain information about  $\rho_{AA}^s$  and  $\rho_{BB}^s$  we first relate them to  $\rho_{AB}^s$ . In Appendix D we use Doi's framework to derive dynamics for  $\rho_{AA}, \rho_{BB}$  from which we derive the following exact equation

$$\begin{aligned} \rho_{AA}^s(t) + \rho_{BB}^s(t) &= (n_A^\infty - n_B^\infty)^2 + 2\rho_{AB}^s(t) \\ &+ 2\lambda \int_0^t dt' S^{(d+1)}(t-t') \rho_{AB}^s(t'). \end{aligned} \quad (54)$$

According to the results of Sections 4, 5 and 6, at long times  $\rho_{AB}^s(t) = \dot{\mathcal{R}}_t / \lambda \sim t^{(1/z)-1}$ . (Note this conclusion followed from assumption 3 and is quite independent of the numerical value of  $\gamma(0)$ .) Substituting this power law in equation (54), using  $S^{(d+1)}(t) \sim t^{-(d+1)/z}$  from equation (16) and incorporating cut-offs in the marginal and non-compact cases (see Eqs. (37, 45, 46)) one sees that the time-dependent terms on the right hand side

of equation (54) tend to zero at long times. Thus, making use of equation (52), we obtain from equation (54)

$$[A(\infty) - 1][n_A^s(\infty)]^2 + [B(\infty) - 1][n_B^s(\infty)]^2 = -2n_A^s(\infty)n_B^s(\infty), \quad (55)$$

where we have defined the unknown functions  $A$  and  $B$  such that  $\rho_{AA}^s(t) \equiv A(t)[n_A^s(t)]^2$  and  $\rho_{BB}^s(t) \equiv B(t)[n_B^s(t)]^2$ . Note that assumptions 4 imply  $A(t), B(t) \geq 1$ ; this in turn implies that the lhs of equation (55) is positive or zero. But the rhs is negative or zero. It follows that *both* sides of this equation must vanish, *i.e.* either or both of  $n_A^s(\infty)$  and  $n_B^s(\infty)$  vanish. But from equation (52),  $n_A^s(\infty) \leq n_B^s(\infty)$ . Hence  $n_A^s(\infty) = 0$  is proved.

## 7.2 Full density field

Having determined that  $n_A^s(\infty)$  vanishes, we return to equations (51) from which we will first determine  $\gamma(0)$  and then calculate the full density profile. Using the expression for  $\tilde{\mathcal{R}}_t(E)$  in equation (27), and making the substitution  $\rho_{AB}^s(E) = \tilde{\mathcal{R}}_t(E)/\lambda$ , equation (51) can be written in Laplace space as

$$n_A(x_A; E) = \frac{n_A^\infty}{E} \left[ 1 - \frac{\lambda n_B^\infty G_E^{(1)}(x_A)}{1 + \lambda S^{(d+1)}(E) + \lambda n_B^\infty \gamma(E) S^{(1)}(E)} \right]. \quad (56)$$

Here the Laplace transform of the propagator  $G_t^{(1)}(x)$  has the following structure:

$$G_E^{(1)}(x) = S^{(1)}(E) \tilde{g}(xE^{1/z}), \quad \tilde{g}(u) \rightarrow \begin{cases} 1 & u \ll 1 \\ 0 & u \gg 1 \end{cases}, \quad (57)$$

where  $\tilde{g}$  is a scaling function with the stated limits. We have used equation (14) and the fact (see Eq. (24)) that  $S^{(1)}(t) = G_t^{(1)}(x=0)$ .

We can now prove  $\gamma(E=0) = 1$ . Consider the limit  $E \rightarrow 0$  of the expression in equation (56) evaluated at  $x_A = 0$ . In this limit the square bracket must vanish since  $n_A^s(t \rightarrow \infty) = 0$ . Now for small enough  $E$ , the many body term  $\lambda n_B^\infty \gamma(E) S^{(1)}(E)$  always dominates over the other two terms 1 and  $\lambda S^{(d+1)}(E)$  (see Eqs. (29, 38, 47)). Thus, using  $G_E^{(1)}(0) = S^{(1)}(E)$ , we must have  $\gamma(0) = 1$ .

Consider now general values of  $x_A, t$  and let us compare the two terms in the brackets on the rhs of equation (56). According to equation (57), the numerator of the 2nd term is less than or equal to the many body term in the denominator; it follows that the quotient can be comparable to 1 only for  $E$  values sufficiently small that the many body term dominates. As we saw in equations (29, 38, 47), this corresponds to times longer than the timescale signifying the crossover from second to first order kinetics. Therefore, retaining leading order terms only in equation (56),

one has

$$n_A(x_A; t) \approx \begin{cases} n_A^\infty & \text{"short" times} \\ n_A^\infty f(x_A/x_t) & t \rightarrow \infty \end{cases} \quad (58)$$

where

$$f\left(\frac{x_A}{x_t}\right) \equiv \mathcal{L}^{-1} \left[ \frac{1 - \tilde{g}(x_A E^{1/z})}{E} \right], \quad f(u) \rightarrow \begin{cases} 0 & u \ll 1 \\ 1 & u \gg 1 \end{cases} \quad (59)$$

and  $\mathcal{L}^{-1}$  denotes inverse Laplace transform. Here by "short" times, we refer to times when second-order kinetics are valid. This completes our calculation of the density profile, which evidently confirms the physical expectations. One sees that at short times  $n_A(x_A; t)$  retains its equilibrium value, whereas at longer times a reactant density depletion hole of size  $x_t$  develops at the interface (see Fig. 3).

As an example of the form of  $f(u)$ , consider small molecules ( $z = 2$ ) for which  $G_t^{(1)}(x)$  is a Gaussian. Determining  $G_E^{(1)}(x_A)$ , one finds from equation (59) that  $f(u) = \text{erf}(u)$ ; this is identical to the asymptotic density profile in the situation in which initially uniformly distributed small molecules adsorb irreversibly onto a surface [17, 18].

## 8 Segregation effects and decay of interfacial density, $n_A^s(t)$

We found in Section 7 that the reactant density at the interface,  $n_A^s(t)$ , tends to zero at long times. In this section we determine the long time power law decay of  $n_A^s(t)$ , considering for simplicity the symmetric case only,  $n_A^\infty = n_B^\infty$ . Interestingly, we will find segregation of reactants into A-rich and B-rich domains at the interface for the compact case.

We begin by establishing time-dependent bounds on  $n_A^s(t)$ . Now assumption 4 will lead to an upper bound of this type, because for the symmetric case  $\rho_{AA}^s(t)$  can be determined from equation (54) since  $\rho_{AB}^s(t)$  is already known. What we need, in addition, is a lower time-dependent bound, which we now introduce by making one further assumption. This assumption is motivated by the physical expectation that the density of A–B interfacial pairs,  $\rho_{AB}^s(t)$ , will never exceed the value it would have if there were no correlations between A and B particles, namely  $[n_A^s(t)]^2$ . That is, A–B reactions will always tend to diminish this pair density relative to the uncorrelated value.

### Assumption 5

There exists a positive finite constant  $b$ , such that:

$$b \rho_{AB}^s(t) \leq [n_A^s(t)]^2 \quad (n_A^\infty = n_B^\infty). \quad (60)$$

### 8.1 Noncompact case ( $d + 1 > z$ )

In Appendix D, equation (D.4), using equation (54) we show that for large enough times  $\rho_{AA}^s(t) \approx (n_A^\infty/\lambda)dx_t/dt$ . Meanwhile, equations (48, 49) imply that  $\rho_{AB}^s(t) \approx (n_A^\infty/\lambda)dx_t/dt$ . Thus the upper and lower long time bounds on  $n_A^s$  implied, respectively, by assumptions 4 and 5 are proportional to the same algebraically decaying function of time. Hence

$$n_A^s(t) \approx \sqrt{\frac{n_A^\infty}{\lambda} \frac{dx_t}{dt}} \sim t^{(1-z)/(2z)} \quad (t \rightarrow \infty, d + 1 > z), \quad (61)$$

up to a (time-dependent) prefactor of order unity.

### 8.2 Compact case ( $d + 1 < z$ )

For this case, as shown in Appendix D, equation (54) leads to the conclusion (see Eq. (D.5)) that asymptotically  $\rho_{AA}^s(t) \approx n_A^\infty x_t^{-d} \sim t^{-d/z}$ . Meanwhile, equations (34, 36) imply the same decay for  $\rho_{AB}^s$  as for the noncompact case,  $\rho_{AB}^s(t) \approx (n_A^\infty/\lambda)dx_t/dt \sim t^{(1-z)/z}$ . Hence the upper and lower bounds on  $n_A^s(t)$  implied by assumptions 4 and 5 involve different power laws:  $n_A^s(t)$  decays at least as slowly as  $t^{-d/(2z)}$  and at least as rapidly as  $t^{(1-z)/(2z)}$ . This is insufficient to determine the actual decay.

We can make progress, however, by invoking the interface analogue of the arguments which were used by Ovchinnikov and Zeldovich [27], and Toussaint and Wilczek [28] to analyze the bulk reaction system  $A + B \rightarrow 0$ . According to this generalization, which we have presented in the introduction, the density of A reactants at the interface cannot decay faster than  $\sqrt{n_A^\infty} x_t^{-d/2} \sim t^{-d/(2z)}$ , which is the rate determined by the decay of fluctuations in the random initial reactant distribution. But we have already shown that  $t^{-d/(2z)}$  is an upper bound. Hence

$$n_A^s(t) \approx \sqrt{n_A^\infty} x_t^{-d/2} \sim t^{-d/(2z)} \quad (t \rightarrow \infty, d + 1 < z). \quad (62)$$

Therefore, the asymptotic density decay at the interface is controlled by the rate of decay of fluctuations. It follows that A-rich and B-rich regions of linear size  $x_t$  develop adjacent to the interface. These are illustrated schematically in Figure 7. An important point to stress is that the long time reaction rate is itself *not* influenced by this segregation, to leading order: the long time reaction rate is governed merely by the fact that  $n_A^s(\infty) = 0$ , whilst segregation effects are associated with higher order terms in  $n_A^s(t)$ , *i.e.* the manner in which  $n_A^s$  decays to zero.

## 9 Discussion

We have shown here that the critical dimension for reaction kinetics at a fixed interface is  $d_c = z - 1$ . This is

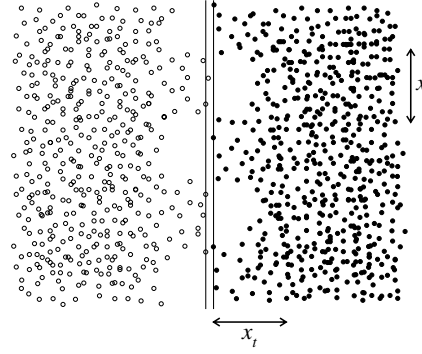


**Fig. 7.** Schematic representation of asymptotic segregation of reactants into A-rich and B-rich domains of size  $x_t$  near to the interface. This segregation occurs only for sufficiently low dimensions,  $d + 1 < z$ .

quite different to the result for reactions at a movable and broadening interface separating 2 *miscible* phases, which problem has been widely studied for the case  $z = 2$  where  $d_c = 2$  has been found [4,5,8,9]. For the fixed interface problem studied here, one has instead  $d_c = 1$ . The difference between these 2 critical dimensions is due to the fact that for the case of miscible reactants, A–B reactions are not restricted to occur only in a  $(d - 1)$ -dimensional plane.

The most novel feature to have emerged from this study is that interfacial reaction kinetics are not of fixed order. This is rather unusual. For example, trimolecular, bimolecular and unimolecular reaction processes are generally governed by 3rd, 2nd and 1st order kinetics, respectively. The peculiar feature here is that 2nd order reaction rate laws are obeyed at short times, whilst 1st order kinetics describe the long time behavior:

$$\begin{aligned} \dot{\mathcal{R}}_t &= k^{(2)} n_A^\infty n_B^\infty \quad (2\text{nd order}), \\ \dot{\mathcal{R}}_t &= k^{(1)} n_A^\infty \quad (1\text{st order}). \end{aligned} \quad (63)$$

The 2nd order coefficient  $k^{(2)}$  may either be a constant (mean field kinetics, MF) or time-dependent (diffusion-controlled kinetics, DC). The time-dependence in the latter case is  $k^{(2)} \approx dx_t^{d+1}/dt$ . In contrast, the 1st order kinetics are always DC, and the 1st order coefficient  $k^{(1)} \approx dx_t/dt$  is always time-dependent.

An important feature of these 1st order kinetics concerns the different roles played by the two far-field reactant densities,  $n_A^\infty$  and  $n_B^\infty$ , in the case where they are unequal. The timescale at which these kinetics onset (either  $t_m^*$  or  $t_l$ ) is determined by the *greatest*,  $n_B^\infty$ . However, the rate law itself involves the *smallest* one,  $n_A^\infty$  (see Eq. (63)). Correspondingly, in the region within a distance  $x_t$  of the interface the density profile falls to a value close to zero on the dilute A side, whereas on the denser B side the profile in this region drops to a finite value close to  $n_B^\infty - n_A^\infty$ .

Apart from our main concern, the reaction rate, this paper has also addressed the evolution of density fields, key features of which are the densities at the interface  $n_A^s, n_B^s$ . This enabled us to examine the validity of the “local mean field” decoupling approximation,

$\dot{\mathcal{R}}_t \approx \lambda n_B^s(t) n_A^s(t)$ , which approximates the densities on either side of the interface to be independent of one another,  $\rho_{AB}^s \approx n_A^s n_B^s$ . In this picture the denser B side is viewed as presenting a uniform “reactive surface” of strength  $\lambda n_B^s(t)$  to the more dilute A reactants. Consider long times, when the diffusive flux of A particles per unit area at the interface is  $n_A^\infty dx_t/dt$ . Equating this to the reaction rate, one sees that the “local mean field” approximation suggests

$$n_A^s(t) \approx \frac{1}{\lambda n_B^s(t)} \frac{dx_t}{dt} n_A^\infty \quad (t \rightarrow \infty, \text{ local mean field approx.}). \quad (64)$$

Now in the symmetric case,  $n_A^s = n_B^s$ , the above result implies  $n_A^s(t) \sim t^{(1-z)/(2z)}$ . But we saw in Section 8 that the decay rate is always limited by the rate at which fluctuations in the initial differences between densities on the A and B side near the interface can diffuse away. This limiting decay was shown to be  $\sim t^{-d/(2z)}$ . This suggests that only in high dimensions,  $d+1 > z$ , is the  $n_A^s(t) \sim t^{(1-z)/(2z)}$  prediction correct; indeed, we demonstrated this in Section 8. We conclude that the local mean field approximation is essentially valid for  $d+1 > z$  at very long times. For all low dimensions  $d+1 < z$ , however, fluctuations determine the decay law:  $n_A^s(t) \sim t^{-d/(2z)}$ , segregation occurs at the interface,  $n_A^s$  and  $n_B^s$  are no longer independent and the the local mean-field approximation is wrong.

Let us make a few comments about the interfacial densities in the asymmetric case,  $n_B^s > n_A^s$ . In this case we expect equation (64) to be valid for *all* dimensions, since  $n_B^s(\infty) = n_B^\infty - n_A^\infty$  is then non-vanishing (see Eq. (52)). Hence the B side will indeed supply a uniform reactive surface for the A reactants. Thus, we expect a different decay law,  $n_A^s \sim t^{(1-z)/z}$  for all dimensions. If the initial reactant densities  $n_A^\infty, n_B^\infty$  are almost but not quite equal to one another, we expect the symmetric case results will be valid up to a cross-over time at which  $n_B^s(t)$  drops to a value close to its asymptotic value,  $n_B^\infty - n_A^\infty$ . Thereafter, equation (64) will correctly describe  $n_A^s$ .

We stress that this study has concerned *irreversible* reactions. Thus an equilibrium state is never attained. The final state will be governed by saturation effects at the interface, which have not been considered here. As  $t \rightarrow \infty$ , in principle a final state will be attained in which reaction product fills every available surface site (in practice, however, the timescale for this state to be reached may be experimentally inaccessible [20,21]).

To conclude, consider a few specific examples. An important parameter determining the class of reaction kinetics is the dimensionless local reactivity,  $Q_b t_a$ . Perhaps the most useful relation to help one estimate its value for a given system is  $Q_b t_a \approx k^{\text{bulk}}/k_{\text{rad}}^{\text{bulk}}$  where  $k^{\text{bulk}} \approx Q_b a^3$  is the bulk rate constant, *i.e.* the 3-dimensional rate constant which would describe A–B reaction kinetics if the molecules could react anywhere within the bulk (see introduction). Here  $k_{\text{rad}}^{\text{bulk}} \approx a^3/t_a \approx 10^9 \text{ l mol}^{-1} \text{ s}^{-1}$  is the same quantity for radicals which are nature’s most reactive chemical species. We assume here the molecular size

$a$  is roughly the same ( $a \approx 3 \text{ \AA}$ ) in all small molecule cases. Thus if one has access to  $k^{\text{bulk}}$  for an A–B system, then one can estimate  $Q_b t_a$ . In the case where the reactive groups are attached to polymer chains,  $k^{\text{bulk}}$  refers of course to the *small molecule* bulk analogue reaction system, *i.e.* the rate constant describing reactions between the same species after removal from their host polymer chains.

### Small molecules: $z = 2, d = 3$

Consider firstly unequal initial bulk densities,  $n_A^\infty \neq n_B^\infty$ . The early 2nd order behavior is non-compact ( $d+1 > z$ ) and MF 2nd order kinetics pertain with  $k^{(2)} = h(Q_b a^3)$ . These continue until  $t_m^* = D/[h(Q_b a^3)n_B^\infty]^2$ , when first order kinetics onset with time-dependent rate constant  $k^{(1)} = D/(Dt)^{1/2}$  where  $D$  is the molecular diffusivity. Note that the cross-over time  $t_m^*$  is determined by the greater of the two far-field densities,  $n_B^\infty$ .

The density profile on the less dense A side is (to leading order) identical to the “reactive surface” situation, having a depletion hole of size  $(Dt)^{1/2}$ . The A density at the interface decays for long times to zero as  $n_A^s \sim 1/t^{1/2}$ . There is no “hole” on the more dense B side, though the density is reduced from its initial value over a region extending  $(Dt)^{1/2}$  into the bulk and has the long time value  $n_B^\infty - n_A^\infty$  at the interface. The symmetric case,  $n_A^\infty = n_B^\infty$ , is different: there are long time holes on both sides and the interfacial density decay is  $n_A^s \sim 1/t^{1/4}$ .

Typical numerical values are  $a \approx h \approx 3 \text{ \AA}$  and  $D \approx 10^{-5} \text{ cm}^2/\text{s}$ . Now for the vast majority of reacting species,  $k^{\text{bulk}} \lesssim 10^3 \text{ l mol}^{-1} \text{ s}^{-1}$ , implying  $t_m^* \gtrsim 10 \text{ s}/\phi_B^2$ , where  $\phi_B = n_B^\infty a^3$  is the far-field volume fraction of B reactants. Thus, depending on the value of  $\phi_B$ , this timescale may become so large that the diffusion-controlled kinetics get washed out by other effects such as convection. For highly reactive species such as radicals, on the other hand, one has  $k^{\text{bulk}} \approx 10^9 \text{ l mol}^{-1} \text{ s}^{-1}$  and  $t_m^* \approx 10^{-10} \text{ s}/\phi_B^2$ ; these kinetics are then observable over a very large range of densities.

### Small molecules in $d = 1$

This is a marginal situation ( $z = d+1$ ) arising in systems where small molecules ( $z = 2$ ) are restricted to an effectively one-dimensional geometry, *e.g.* molecules trapped in a thin tube.

For highly reactive species,  $Q_b t_a \approx 1$  (*i.e.*  $k^{\text{bulk}} \approx k_{\text{rad}}^{\text{bulk}}$ ) the initial regime is 2nd order with a weakly time-dependent rate constant  $k^{(2)} \approx D/\ln(t/t_h)$ . At time  $T_l = D^{-1}(n_B^\infty)^{-2}[\ln(n_B^\infty h)^2]^2$  first order kinetics onset with time-dependent  $k^{(1)} = D/(Dt)^{1/2}$ .

For most cases, however, the local dimensionless reactivity  $Q_b t_a$  will be below a very high threshold value (*i.e.* very close to unity) given by  $Q_b^* t_a = (a/h)/[\ln(n_B^\infty h)^2]^2$ . In such cases an initial 2nd order mean field regime with

$k^{(2)} = Q_b h a = k^{\text{bulk}} h/a^2$  is followed at time  $t_m^* = t_a/(Q_b t_a n_B^\infty h)^2$  by the same 1st order kinetics. In all cases a depletion hole of size  $(Dt)^{1/2}$  grows at long times on the dilute A side.

### Unentangled polymers, short times: $z = 4$ , $d = 3$

Consider an interface separating two immiscible unentangled polymer melts comprising chains with degree of polymerization  $N$  and radius of gyration  $R$ , each carrying one reactive group. Thus the density of reactive groups is  $n_A^\infty = n_B^\infty = 1/(Na^3)$  or equivalently  $\phi_A = \phi_B = 1/N$ . Then Rouse dynamics apply [25,26],  $x_t \approx R(t/\tau)^{1/4}$  for times less than the single chain longest relaxation time,  $\tau \approx t_a N^2$ . Thus, for  $t < \tau$ , we are in the marginal situation  $z = d + 1 = 4$ .

Consider first the maximally reactive case  $Q_b t_a = 1$ . Initially kinetics are 2nd order with weakly time-dependent rate constant  $k^{(2)} = (R^4/\tau)/\ln(t/t_h)$ . The cross over to first order kinetics, with  $k^{(1)} \approx (R/\tau)(t/\tau)^{-3/4}$ , occurs at  $T_l = t_a \phi_B^{-4/3} \ln(\phi_B^{-4/3} a^4/h^4)$ . For typical values  $h/a = 5$ ,  $N = 200$  one has  $T_l \approx 0.02 \tau$ .

For less reactive species,  $Q_b t_a < Q_b^* t_a$  where  $Q_b^* t_a \approx a/[h \ln(\phi_B^{-4/3} a^4/h^4)]$ , the kinetics are different. (For the above typical numerical values,  $Q_b^* t_a \approx 0.7$ .) In this case second order MF kinetics with  $k^{(2)} = h(Q_b a^3)$  are followed at  $t_m^* = t_a [Q_b (h/a) t_a \phi_B]^{-4/3}$  by 1st order kinetics with  $k^{(1)} = (R/\tau)(t/\tau)^{-3/4}$ .

In both of these examples, a long time depletion hole grows on the dilute A side whose size increases in time as  $x_t \approx R(t/\tau)^{1/4}$ .

### Entangled polymers, “breathing” modes: $z = 8$ , $d = 3$

Consider the same polymer example as above, but now chains are entangled. Using the reptation model to describe the polymer dynamics, let us ask what reaction kinetics are during the short time “breathing modes” regime ( $t_e < t < t_b$ ) when [25,26]  $x_t = r_e(t/t_e)^{1/8}$ . Here  $t_e = N_e^2 t_a$  is the entanglement time ( $N_e$  being the entanglement threshold),  $t_b = (N/N_e)^2 t_e$  is the Rouse time for the one-dimensional tube motion and  $r_e = N_e^{1/2} a$  is the tube diameter. This is an interesting example of a compact case,  $d + 1 < z = 8$ .

Consider very reactive groups such as radicals,  $Q_b t_a \approx 1$ , and  $n_B^\infty$  values such that  $t_l$  (the diffusion time corresponding to a distance equal to the typical separation between the B reactive groups) satisfies  $t_e < t_l < t_b$ . Then  $t_l = t_e (n_B^\infty r_e^3)^{-8/3}$ . Now for  $t > t_e$  there is no MF regime and kinetics are 2nd order DC,  $k^{(2)} \approx (r_e^4/t_e)(t/t_e)^{-1/2}$ . For  $t > t_l$  the kinetics become 1st order with  $k^{(1)} = (r_e/t_e)(t/t_e)^{-7/8}$  and a depletion hole grows on the A side of size  $\sim t^{1/8}$ .

As a specific example, if all B-chains carry one reactive end-group ( $n_B^\infty a^3 = 1/N$ ) and  $N \approx 10^4$ ,  $N_e \approx 200$  one has  $t_l \approx 30 t_e \approx 10^{-3} t_b$ . Thus both 2nd and 1st order kinetics as described above will occur within the  $t^{1/8}$  regime.

This work was supported by the National Science Foundation under grant No. DMR-9403566. We thank Uday Sawhney for stimulating discussions.

## Appendix A: Derivation for $z = 2$ of dynamical equations for 2-body and 1-body density correlation functions

In this Appendix we employ the second-quantization formalism for classical many-particle systems developed by Doi [42] to derive exact evolution equations, in the case of small molecules ( $z = 2$ ), obeyed by the 2-body correlation functions  $\rho_{AB}, \rho_{AA}, \rho_{BB}$  and the density fields  $n_A, n_B$ . We do not attempt here a self-contained discussion of the Doi formalism: the reader is referred to Doi’s papers, reference [42], for the necessary background.

In the Doi formalism any physical quantity  $A$  is mapped onto a quantum operator  $\tilde{A}$  given in terms of the Bose creation and annihilation operators. For systems consisting of two types of particles, A and B, there are two types of Bose operators,  $\psi_A(\mathbf{r}), \psi_B(\mathbf{r})$ , for every spatial location  $\mathbf{r}$ . These satisfy the following commutation relations

$$\begin{aligned} [\psi_\nu(\mathbf{r}), \psi_\mu^\dagger(\mathbf{r}')] &= \delta(\mathbf{r} - \mathbf{r}') \delta_{\nu\mu}, \\ [\psi_\nu^\dagger(\mathbf{r}), \psi_\mu^\dagger(\mathbf{r}')] &= [\psi_\nu(\mathbf{r}), \psi_\mu(\mathbf{r}')] = 0, \end{aligned} \quad (\text{A.1})$$

where  $\nu = A, B$  and  $\mu = A, B$ . The dynamics of  $A(t)$  are determined by a quantum propagator  $\tilde{G}$ ,

$$A(t) = \langle 1 | \tilde{A} e^{-\tilde{G}t} | c \rangle. \quad (\text{A.2})$$

Here,  $\langle 1 | \equiv \langle 0 | \exp[\int d\mathbf{r}_A \psi_A(\mathbf{r}_A) \int d\mathbf{r}_B \psi_B(\mathbf{r}_B)]$  is a coherent state,  $\langle 0 |$  is the vacuum state and  $\langle 1 | \psi_A^\dagger(\mathbf{r}) = \langle 1 | \psi_B^\dagger(\mathbf{r}) = \langle 1 |$ . The quantum state  $|c\rangle$  represents the initial state of the system; although its form will not be relevant in the subsequent calculations, we remark that in the case where A and B particles are initially randomly distributed with densities  $n_A^\infty$  and  $n_B^\infty$  then  $|c\rangle = \exp[n_A^\infty n_B^\infty \int d\mathbf{r}_A \psi_A^\dagger(\mathbf{r}_A) \int d\mathbf{r}_B \psi_B^\dagger(\mathbf{r}_B)] |0\rangle$ .

In the present reaction-diffusion interface problem, the propagator  $\tilde{G} = \tilde{G}_0 + \tilde{G}_r$  consists of a “diffusion” part,  $\tilde{G}_0$ , and a “reaction” part,  $\tilde{G}_r$ . For small molecules obeying simple Fickian diffusion, according to Doi [42]

$$\begin{aligned} \tilde{G}_0 &= -D \int d\mathbf{r}_A \psi_A^\dagger(\mathbf{r}_A) \nabla_A^2 \psi_A(\mathbf{r}_A) \\ &\quad - D \int d\mathbf{r}_B \psi_B^\dagger(\mathbf{r}_B) \nabla_B^2 \psi_B(\mathbf{r}_B). \end{aligned} \quad (\text{A.3})$$

The reaction part,  $\tilde{G}_r$ , is constructed [42] from the reaction sink function which in our model is  $\lambda \delta(x_A) \delta(\mathbf{r}_A - \mathbf{r}_B)$ . We find that the corresponding quantum operator is

$$\begin{aligned} \tilde{G}_r &= \lambda \int d\mathbf{r}^T \left\{ \psi_A^\dagger(\mathbf{r}^T) \psi_B^\dagger(\mathbf{r}^T) \psi_A(\mathbf{r}^T) \psi_B(\mathbf{r}^T) \right. \\ &\quad \left. - \psi_A(\mathbf{r}^T) \psi_B(\mathbf{r}^T) \right\}. \end{aligned} \quad (\text{A.4})$$

The two annihilation operators in the second term in  $\tilde{G}_r$  are responsible for reactions between A–B pairs in contact at the interface, while the first part is necessary to ensure proper normalization of averages [42].

Differentiating equation (A.2), and using the identity  $\langle 1 | \tilde{G} = 0$  which follows from the above definition of  $\tilde{G}$ , one has

$$\frac{dA(t)}{dt} = \langle 1 | [\tilde{G}, \tilde{A}] e^{-\tilde{G}t} | c \rangle. \quad (\text{A.5})$$

We can now derive the dynamical equations obeyed by the correlation functions from equation (A.5). The operator representations of the many-body correlation functions are [42] as follows:

$$\begin{aligned} \tilde{n}_\nu(\mathbf{r}) &= \psi_\nu^\dagger(\mathbf{r})\psi_\nu(\mathbf{r}), \\ \tilde{\rho}_{\mu\nu}(\mathbf{r}, \mathbf{r}') &= \psi_\nu^\dagger(\mathbf{r})\psi_\mu^\dagger(\mathbf{r}')\psi_\nu(\mathbf{r})\psi_\mu(\mathbf{r}'), \\ \tilde{\rho}_{\sigma\mu\nu}(\mathbf{r}, \mathbf{r}', \mathbf{r}'') &= \psi_\sigma^\dagger(\mathbf{r})\psi_\mu^\dagger(\mathbf{r}')\psi_\nu^\dagger(\mathbf{r}'')\psi_\sigma(\mathbf{r})\psi_\mu(\mathbf{r}')\psi_\nu(\mathbf{r}'') \\ &\quad (\sigma, \mu, \nu = A, B). \end{aligned} \quad (\text{A.6})$$

From equation (A.5), with  $A = n_A$  and  $\tilde{A} = \tilde{n}_A$ , and using the above representation for  $\tilde{n}_A$ , one obtains

$$\begin{aligned} \frac{dn_A(\mathbf{r}_A; t)}{dt} &= D\nabla_A^2 \langle 1 | \psi_A^\dagger(\mathbf{r}_A)\psi_A(\mathbf{r}_A)e^{-\tilde{G}t} | c \rangle \\ &\quad - \lambda\delta(x_A) \langle 1 | \psi_A^\dagger(\mathbf{r}_A^T)\psi_B^\dagger(\mathbf{r}_A^T)\psi_A(\mathbf{r}_A^T)\psi_B(\mathbf{r}_A^T)e^{-\tilde{G}t} | c \rangle \end{aligned} \quad (\text{A.7})$$

after using the commutation relations of equation (A.1) and the properties of the coherent state  $\langle 1 |$ . From equations (A.6, A.2) one recognizes this as the first of equations (50) in the main text (dynamics of  $n_A, n_B$ ). Notice that the commutation of  $\tilde{G}$  with  $\tilde{n}$  in equation (A.5) produced, among other quantities, a higher order correlation function; this is the origin of the hierarchical structure of the reaction-diffusion equations.

Performing a similar analysis for the 2-body correlation functions (setting  $A = \rho_{\mu\nu}$  and  $\tilde{A} = \tilde{\rho}_{\mu\nu}$ ) one obtains equations (12) (dynamics of  $\rho_{AB}$ ) and equation (D.1) (dynamics of  $\rho_{AA}, \rho_{BB}$ ).

## Appendix B: Proof that relative contribution of region I to $I_m^A(t)$ is order unity

We saw in Section 3 that the many-body integral term  $I_m^A(t)$  involving  $\rho_{BAB}(\mathbf{r}|0, 0; t)$  in equation (19) receives contributions from two space-time regions, I and II. In this appendix we demonstrate that the contribution from region I is a fraction of order unity of the value of  $I_m^A(t)$  itself. We show this by firstly deriving an upper bound on  $I_m^A(t)$ . Then we derive a lower bound on  $I_m^A(t)$  corresponding to  $\rho_{BAB}$  being zero in region II and having its minimum value in region I. The lower and upper bounds will then be shown to be of the same order, proving the

desired result. These bounds are all consequences of assumptions 1, 2 and 3 (see main text).

From assumption 1 one sees that the substitution  $\rho_{BAB}(\mathbf{r}'_B|0, 0; t) \rightarrow Un_B^\infty$  in the expression for  $I_m^A(t)$  (Eq. (19)) defines an upper bound on  $I_m^A(t)$ ,

$$I_m^A(t) \leq Un_B^\infty \int_0^t dt' S^{(1)}(t-t') \rho_{AB}^s(t'), \quad (\text{B.1})$$

where we have used equation (13) to perform the integration.

Now assumption 2 implies that

$$\rho_{BAB}(\mathbf{r}'_B|0, 0; t') \geq \begin{cases} Ln_B^\infty & x'_B/x_{t'} > 1, \text{ region I} \\ 0 & x'_B/x_{t'} < 1, \text{ region II} \end{cases} \quad (\text{B.2})$$

Substituting the above lower bound on  $\rho_{BAB}$  in the expression for  $I_m^A(t)$  of equation (19), we obtain the following lower bound on  $I_m^A(t)$

$$I_m^A(t) \geq Ln_B^\infty \int_0^t dt' \frac{1}{x_{t-t'}} \rho_{AB}^s(t') \int_{\xi_x > (x_{t'}/x_{t-t'})} d^d \xi h(\xi), \quad (\text{B.3})$$

where we have used the following scaling structure for the function  $F_t(\mathbf{r}'_B)$  appearing in the expression for  $I_m^A(t)$  of equation (19),

$$F_t(\mathbf{r}'_B) = \frac{1}{x_t^{d+1}} h\left(\frac{\mathbf{r}'_B}{x_t}\right), \quad h(\mathbf{u}) \rightarrow \begin{cases} 1 & u \ll 1 \\ 0 & u \gg 1 \end{cases}. \quad (\text{B.4})$$

This follows from equation (14). The integration variable in equation (B.3) is  $\xi = \mathbf{r}'_B/x_{t-t'}$  and  $\xi_x$  denotes the component of  $\xi$  orthogonal to the interface.

Now using equation (B.4), there exists a positive constant  $E$  of order unity such that

$$\int_{\xi_x > (x_{t'}/x_{t-t'})} d^d \xi h(\xi) \geq \begin{cases} E & (x_{t'}/x_{t-t'} < 1 \text{ or } t' < t/2) \\ 0 & (x_{t'}/x_{t-t'} > 1 \text{ or } t' > t/2) \end{cases}. \quad (\text{B.5})$$

Expression (B.5) in inequality (B.3) implies that

$$I_m^A(t) \geq ELn_B^\infty \int_0^{t/2} dt' \frac{1}{x_{t-t'}} \rho_{AB}^s(t'). \quad (\text{B.6})$$

Notice that according to equation (16),  $S^{(1)}(t) \approx 1/x_t$ . Therefore, inequality (B.6) is very close to showing that the lower bound on  $I_m^A(t)$  is of the same order as the upper bound in equation (B.1), except for the fact that the time integral on the right hand side of this inequality has upper limit  $t/2$  rather than  $t$ . However, if one makes the replacement  $t/2 \rightarrow t$  for this upper limit, this yields

the same result to within a constant of order unity. This is a consequence firstly of the fact that since  $z > 1$  in equation (1) thus both  $\int_0^{t/2} dt'/x_{t-t'}$  and  $\int_{t/2}^t dt'/x_{t-t'}$  are of the same order, and secondly that  $\rho_{AB}^s(t')$ , according to assumption 3, is a decreasing function of time.

Thus we have shown that the upper and lower bounds on  $I_m^A(t)$  are of the same order. But the crucial point is that the lower bound on  $I_m^A(t)$  of equation (B.3) results from an integration receiving *zero* contribution from region II and minimal contribution from region I. It follows that the actual contribution from region I must be of the same order as the actual value of  $I_m^A(t)$ .

## Appendix C: Inverse Laplace transform of $1/(E \ln E)$

We show in this appendix that

$$\mathcal{L}^{-1} \left[ \frac{-1}{E \ln(Et_h)} \right] = \frac{1}{\Gamma(1) \ln(t/t_h)} \quad (t \gg t_h), \quad (\text{C.1})$$

where  $\mathcal{L}^{-1}$  denotes inverse Laplace transform. Now it is well-known that

$$\mathcal{L}^{-1} \left[ \frac{1}{(Et_h)^n} \right] = \frac{t^{n-1}}{t_h^n \Gamma(n)} \quad (n > 0). \quad (\text{C.2})$$

Integrating both sides of equation (C.2) with respect to  $n$  from  $n = 0$  to  $n = 1$  then gives

$$\mathcal{L}^{-1} \left[ \left( 1 - \frac{1}{Et_h} \right) \frac{1}{\ln Et_h} \right] = \frac{1}{t} \int_0^1 \frac{e^{n \ln(t/t_h)}}{\Gamma(n)} dn. \quad (\text{C.3})$$

The function  $1/\Gamma(n)$  is finite for all  $n$  in  $[0, 1]$ . Thus, expanding  $1/\Gamma(n)$  in a Taylor series around  $n = 1$  in the integral on the rhs of equation (C.3), we obtain

$$\frac{1}{t} \int_0^1 \frac{e^{n \ln(t/t_h)}}{\Gamma(n)} dn = \frac{1}{\Gamma(1) t_h \ln(t/t_h)} + O \left( \frac{1}{t_h [\ln(t/t_h)]^2} \right) \quad (t \gg t_h). \quad (\text{C.4})$$

Considering the limit  $t \gg t_h$ , corresponding to  $Et_h \ll 1$ , from equations (C.3, C.4) we deduce equation (C.1).

## Appendix D: Like particle correlation functions $\rho_{AA}, \rho_{BB}$ : asymptotic decay and proof of equation (55)

Using Doi's second-quantization formalism [42] it is shown in Appendix A that for  $z = 2$  (small molecules)  $\rho_{AA}(\mathbf{r}_A, \mathbf{r}'_A; t)$  and  $\rho_{BB}(\mathbf{r}_B, \mathbf{r}'_B; t)$  obey the following

dynamics

$$\begin{aligned} \left\{ \frac{\partial}{\partial t} - D [\nabla_{\mathbf{r}_A}^2 + \nabla_{\mathbf{r}'_A}^2] \right\} \rho_{AA}(\mathbf{r}_A, \mathbf{r}'_A; t) = & \\ & - \lambda \delta(x_A) \rho_{AAB}(\mathbf{r}_A, \mathbf{r}'_A, \mathbf{r}_A; t) \\ & - \lambda \delta(x'_A) \rho_{AAB}(\mathbf{r}_A, \mathbf{r}'_A, \mathbf{r}'_A; t) \\ \left\{ \frac{\partial}{\partial t} - D [\nabla_{\mathbf{r}_B}^2 + \nabla_{\mathbf{r}'_B}^2] \right\} \rho_{BB}(\mathbf{r}_B, \mathbf{r}'_B; t) = & \\ & - \lambda \delta(x_B) \rho_{BBA}(\mathbf{r}_B, \mathbf{r}'_B, \mathbf{r}_B; t) \\ & - \lambda \delta(x'_B) \rho_{BBA}(\mathbf{r}_B, \mathbf{r}'_B, \mathbf{r}'_B; t). \end{aligned} \quad (\text{D.1})$$

Equations (D.1) have a similar form to equation (12) for the  $\rho_{AB}(\mathbf{r}_A, \mathbf{r}_B; t)$  dynamics except that the two-body sink term responsible for pair reactions in equation (12) is absent since two particles of the same species cannot react with one another. Solving equations (D.1) and setting  $\mathbf{r}_A, \mathbf{r}'_A, \mathbf{r}_B, \mathbf{r}'_B = 0$  we obtain

$$\begin{aligned} \rho_{AA}^s(t) &= (n_A^\infty)^2 - 2\lambda I_m^B(t), \\ \rho_{BB}^s(t) &= (n_B^\infty)^2 - 2\lambda I_m^A(t), \end{aligned} \quad (\text{D.2})$$

where  $I_m^A(t), I_m^B(t)$  are defined in equation (17) of Section 2 and are the identical many-body integral expressions which appeared in the solution for  $\rho_{AB}^s$  of equation (15).

Using the above expressions for the like interfacial pair densities together with equation (15) for  $\rho_{AB}^s$ , one obtains the exact relation displayed in equation (54). This result tells us we can determine the sum  $\rho_{AA}^s(t) + \rho_{BB}^s(t)$  from knowledge of  $\rho_{AB}^s(t)$ . For general  $z$ , equation (54) remains valid, provided one replaces everywhere the Gaussian  $z = 2$  propagator with the propagator  $G_t$  appropriate to the dynamics.

Consider the symmetric case,  $\rho_{AA}^s(t) = \rho_{BB}^s(t)$ . Laplace transforming equation (54) we obtain

$$\rho_{AA}^s(E) = \rho_{AB}^s(E) \left\{ 1 + \lambda S^{(d+1)}(E) \right\} \quad (n_A^\infty = n_B^\infty). \quad (\text{D.3})$$

In the non-compact case ( $d + 1 > z$ ), from equations (45, 46), according to which  $S^{(d+1)}(E)$  is a constant, and from the asymptotic form of  $\rho_{AB}^s(t) = \dot{\mathcal{R}}_t/\lambda \sim t^{1/z-1}$  (see Eqs. (48, 49)) one has

$$\rho_{AA}^s(t) \approx \begin{cases} \left\{ (1 + \lambda t_h/h^{d+1})/\lambda \right\} n_A^\infty dx_t/dt & z < d + 1 < z + 1 \\ \left\{ (1 + Q_b t_a)/\lambda \right\} n_A^\infty dx_t/dt & d > z \end{cases} \quad (n_A^\infty = n_B^\infty, t \rightarrow \infty). \quad (\text{D.4})$$

Meanwhile in the compact case, from equation (16) one has  $S^{(d+1)}(E) \sim E^{(d+1)/z-1}$ ; thus, using  $\rho_{AB}^s(E) = \dot{\mathcal{R}}_t(E)/\lambda \sim E^{-1/z}$  from equation (29), valid for  $E \rightarrow 0$ , one has from equation (D.3)

$$\rho_{AA}^s(t) \approx n_A^\infty x_t^{-d} \sim t^{-d/z} \quad (d < z, n_A^\infty = n_B^\infty, t \rightarrow \infty). \quad (\text{D.5})$$

## References

1. G. Astarita, *Mass Transfer with Chemical Reaction* (Elsevier, New York, 1967).
2. L.K. Doraiswamy, M.M. Sharma, *Heterogeneous Reactions: Analysis, Examples, and Reactor Design* (John Wiley & Sons, New York, 1984), Vol. 1: Gas-Solid and Solid-Solid Reactions, Vol. 2: Fluid-Fluid-Solid Reactions.
3. L. Gálfi, Z. Rácz, *Phys. Rev. A* **38**, 3151 (1988).
4. S. Cornell, M. Droz, B. Chopard, *Phys. Rev. A* **44**, 4826 (1991).
5. S. Cornell, M. Droz, *Phys. Rev. Lett.* **70**, 3824 (1993).
6. M. Araujo, H. Larralde, S. Havlin, H.G. Stanley, *Phys. Rev. Lett.* **71**, 3592 (1993).
7. H. Taitelbaum, S. Havlin, J.E. Kiefer, B. Trus, G.H. Weiss, *J. Stat. Phys.* **65**, 873 (1991).
8. B.P. Lee, J. Cardy, *Phys. Rev. E* **50**, R3287 (1994).
9. M. Howard, J. Cardy, *J. Phys. A* **28**, 3599 (1995).
10. G.T. Barkema, M. Howard, J. Cardy, *Phys. Rev. E* **53**, R2017 (1996).
11. Y.-E.L. Koo, R. Kopelman, *J. Stat. Phys.* **65**, 893 (1991).
12. M. Okamoto, T. Inoue, *Polymer Eng. Sci.* **33**, 175 (1993).
13. U. Sundararaj, C. Macosko, *Macromolecules* **28**, 2647 (1995).
14. E. Kramer, L.J. Norton, C.-A. Dai, Y. Sha, C.-Y. Hui, *Faraday Discuss.* **98**, 31 (1994).
15. D. Gersappe, D. Irvine, A.C. Balazs, Y. Liu, J. Sokolov, M. Rafailovich, S. Schwarz, D.G. Peiffer, *Science* **265**, 1072 (1994).
16. S.T. Milner, H. Xi, *J. Rheol.* **40**, 663 (1996).
17. H.S. Carslaw, J.C. Jaeger, *Conduction of Heat in Solids*, 2nd edn. (Clarendon Press, Oxford, 1959).
18. O. Bychuk, B. O'Shaughnessy, *J. Colloid Interf. Sci.* **167**, 193 (1994).
19. C.J. Durning, B. O'Shaughnessy, *J. Chem. Phys.* **88**, 7117 (1988).
20. B. O'Shaughnessy, U. Sawhney, *Phys. Rev. Lett.* **76**, 3444 (1996).
21. B. O'Shaughnessy, U. Sawhney, *Macromolecules* **29**, 7230 (1996).
22. G.H. Fredrickson, *Phys. Rev. Lett.* **76**, 3440 (1996).
23. G.H. Fredrickson, S.T. Milner, *Macromolecules* **29**, 7386 (1996).
24. B. O'Shaughnessy, D. Vavylonis, cond-mat/9804091 (to appear in *Phys. Rev. Lett.*).
25. M. Doi, S.F. Edwards, *The Theory of Polymer Dynamics* (Clarendon Press, Oxford, 1986).
26. P.G. de Gennes, *Scaling Concepts in Polymer Physics* (Cornell Univ. Press, Ithaca, New York, 1985).
27. A.A. Ovchinnikov, Y.B. Zeldovich, *Chem. Phys.* **28**, 215 (1978).
28. D. Toussaint, F. Wilczek, *J. Chem. Phys.* **78**, 2642 (1983).
29. P. Meakin, H.E. Stanley, *J. Phys. A* **17**, L173 (1984).
30. K. Kang, S. Redner, *Phys. Rev. A* **32**, 435 (1985).
31. B.P. Lee, J. Cardy, *J. Stat. Phys.* **80**, 971 (1995).
32. B. O'Shaughnessy, *Phys. Rev. Lett.* **71**, 3331 (1993); *Macromolecules* **27**, 3875 (1994).
33. M. Doi, *Chem. Phys.* **11**, 115 (1975).
34. P.G. de Gennes, *J. Chem. Phys.* **76**, 3316 (1982); *ibid.* 3322 (1982).
35. B. O'Shaughnessy, D. Vavylonis, *Europhys. Lett.* **45**, 653 (1999).
36. B. Friedman, B. O'Shaughnessy, *Macromolecules* **26**, 5726 (1993).
37. A.L.J. Beckwith, S. Brumby, R.F. Claridge, R. Crocket, E. Roduner, in *Radical Reaction Rates in Liquids*, edited by H. Fischer (Springer-Verlag, Berlin, 1994), Vol. 18, Subvol. a of Landolt-Börnstein Numerical Data and Functional Relationships in Sciences and Technology, New Series, Group II, Atomic and Molecular Physics.
38. I. Mita, K. Horie, *J. Macromol. Sci. Rev. Macromol. Chem. Phys. C* **27**, 91 (1987).
39. E.T. Denisov, *Liquid-Phase Reaction Rate Constants* (IFI/Plenum, New York, 1974).
40. *Investigation of Rates and Mechanisms of Reactions*, 4th edn., edited by C.L. Bernasconi (John Wiley & Sons, New York, 1986), Vol. VI: Techniques of Chemistry.
41. E. Kotomin, V. Kuzovkov, *Modern Aspects of Diffusion-Controlled Reactions; Cooperative phenomena in Bimolecular processes*, edited by R.G. Compton, G. Hancock (Elsevier, Amsterdam, 1996), Vol. 34: Comprehensive Chemical Kinetics.
42. M. Doi, *J. Phys. A* **9**, 1465 (1976); *ibid.* 1479 (1976).
43. B. Friedman, G. Levine, B. O'Shaughnessy, *Phys. Rev. A* **46**, R7343 (1992).
44. B.P. Lee, *J. Phys. A* **27**, 2633 (1994).
45. Y.B. Zel'dovich, A.A. Ovchinnikov, *Zh. Eksp. Teor. Fiz.* **74**, 1588 (1978).
46. B. Friedman, B. O'Shaughnessy, *Phys. Rev. Lett.* **60**, 64 (1988).
47. B. O'Shaughnessy, *J. Chem. Phys.* **94**, 4042 (1991).